

THE DYNAMIC BEHAVIOR OF DOMAIN WALLS
IN BARIUM TITANATE

by

Elizabeth Alden Little

B.A., Wellesley College
(1948)

SUBMITTED IN PARTIAL FULFILLMENT OF THE
REQUIREMENTS FOR THE DEGREE OF
DOCTOR OF PHILOSOPHY

at the

MASSACHUSETTS INSTITUTE OF TECHNOLOGY
September, 1954

Signature redacted

Signature of Author
Department of Physics, August 23, 1954

Signature redacted

Certified by
Thesis Supervisor

Signature redacted

Accepted by
Chairman, Departmental Committee
on Graduate Students

✓

ABSTRACT

THE DYNAMIC BEHAVIOR OF DOMAIN WALLS
IN BARIUM TITANATE

by

Elizabeth Alden Little

Submitted to the Department of Physics on August 23, 1954 in partial fulfillment of the requirements for the degree of Doctor of Philosophy.

The nucleation and growth of 180° (antiparallel) domains and 90° domains in barium titanate single crystals have been measured with optical techniques.

The creation of 180° domains proceeds by the nucleation of long thin spikes with an initial velocity along the polar axis of about 10⁴ cm/sec, for E = 5 kv/cm. As neutralizing electric charges accumulate at the domain walls, the spike widens to form a wedge-shaped domain and the total switching time is determined by the slow growth velocity of such space charge compensated wedges.

The growth of 90° domains in an electric field also begins by the nucleation of long thin wedges. Direct measurements of the nucleation rate as a function of time and field strength show that this rate traverses a maximum as a function of time. The maximum growth rate of a single wedge approaches asymptotically about 10⁶ cm/sec with increasing fields. After a 90° domain has been introduced into a single domain crystal, its growth may be described in terms of the sideways motion of 90° walls. The displacement of a 90° wall is strongly dependent on strains and the state of clamping of the crystal, and wall motion appears to cease for frequencies in the megacycle range, where the piezoelectric resonances of the whole crystal set in.

The differences between 180° and 90° wall motion are related to the wall structure and thereby to the wall thickness and energy, both of which are lower for the 180° than for the 90° wall.

The interaction of 90° and 180° domains has also been investigated. By the growth of 180° domains, 90° walls may become head-to-head or tail-to-tail walls. Such interactions lead to notably long relaxation times.

Finally, the rotation of the optical axes of single domains in electric fields has been measured. A quantitative discussion of this experiment has been based on an expansion of the shear terms in Devonshire's equation for the free energy of the ferroelectric crystal, and an approximate value for the energy of a 90° wall has been derived.

Thesis Supervisor: A. R. von Hippel

Title: Professor of Electrophysics

Handwritten (Phys) Dec 2, 1954

ACKNOWLEDGMENT

The author wishes to express her appreciation to Professor A. R. von Hippel for suggesting the problem and for his advice and encouragement during the course of this research.

She also wishes to thank Dr. P. W. Forsbergh, Jr. for an introduction to the intricacies of domain patterns in barium titanate crystals and for many illuminating discussions.

Particular gratitude is expressed to Professor F. R. Kotter for the use of his rectangular pulse generator, and to Professor H. E. Edgerton for the use of a stroboscopic light.

The author acknowledges gratefully the assistance of W. Westphal in obtaining the dielectric measurements, and of L. E. Johnson, B. Frackiewicz, and Professor D. J. Epstein in the electrical instrumentation.

The author wishes to express her gratitude to the International Business Machines Corp. for support in the form of a fellowship, as well as to Dr. D. R. Young of I.B.M. for many informative discussions.

TABLE OF CONTENTS

	<u>Page</u>
ABSTRACT	1
ACKNOWLEDGMENT	2
TABLE OF CONTENTS	3
I. INTRODUCTION	5
II. EXPERIMENTAL PROCEDURES	9
Preparation of Crystals	9
Microscopic Techniques	11
Electrical Instrumentation	12
III. ANTIPARALLEL DOMAINS	15
Nucleation and Initial Motion	17
Discussion	20
Reversal of the Saturation Polarization by Antiparallel Domains	21
Dielectric Measurements on 180° Walls	27
Summary for 180° Domains	29
IV. 90° DOMAINS	31
Nucleation of 90° Domains	34
90° Wall Motion	40
Discussion	46
V. DOMAIN INTERACTION	47
Wall Motion in DC Fields	50
Wall Motion for Square Pulses	55
Wall Motion in AC Fields	58
Temperature Effects	62
VI. ADDITIONAL OBSERVATIONS	65
Rotation of Optical Axis	65
Cubic-Tetragonal Domains	67
Fatigue	68
VII. DISCUSSION	70
Nucleation and Growth of 90° Domains	71
Nucleation and Growth of 180° Domains	75
Some General Observations	78
VIII. SUMMARY	80
APPENDIX A: ELECTRICAL, MECHANICAL, AND OPTICAL RELATIONS.	81
Rotation of Optical Axis	81
Rotation of Polar Axis and Elastic Shear	82
Free Energy for Rotation	86
Simplified Free Energy for Rotation	88

	<u>Page</u>
APPENDIX B: WALL ENERGY	92
90° Wall Energy	92
180° Wall in a Field Normal to the Wall	93
LIST OF FIGURES AND ILLUSTRATIONS	95
BIBLIOGRAPHY	97
BIOGRAPHICAL NOTE	99

I. INTRODUCTION

Barium titanate is a material with remarkable properties. First reported in 1942 by Wainer and Salomon (1) as having unusual dielectric characteristics, it revealed uncommon electrical, mechanical and optical properties in rapid succession. Investigations performed at the Laboratory for Insulation Research by von Hippel and co-workers (2,3) and shortly thereafter in Russia by Wul and co-workers (4), established barium titanate as a new ferroelectric material. At the Curie point near 120°C , a phase transition from cubic to tetragonal occurs (5) and hysteresis loops develop; at room temperature the c/a ratio has reached about 1.01. Two additional phase transitions are observed near 0°C and -80°C (2,3). The ceramic when prepolarized, is strongly piezoelectric (6).

With the discovery of a method of growing good crystals from ternary melts (7,8), measurements on single crystals were made possible. The several phases can be characterized as follows (9,10). Above 120°C the crystal is cubic with no spontaneous polarization. Below 120° a spontaneous polarization, P_s , of about 0.26 coul./m^2 * develops. From 120°C to 0°C , P_s is directed along a $\langle 100 \rangle$ direction, from 0°C to -80°C along a $\langle 110 \rangle$ direction, and below -80°C along a $\langle 111 \rangle$ direction of the original cube. In each case the mechanical deformation of the lattice is proportional to the square of the polarization: expansion takes

*MKS units will be used.

place in the direction of the polarization and contraction at right angles to it. It follows that as the temperature is lowered from above 120°C, the crystal symmetry changes successively from cubic, O_h , to tetragonal, C_{4v} , to orthorhombic, C_{2v} , to rhombohedral, C_{3v} (11).

In the tetragonal phase with which the present study is concerned, the optical ellipsoid is uniaxial negative (9) and the birefringence, $n_c - n_a$, where n_c and n_a are the indices of refraction along the a and c axes respectively, is proportional to the mechanical deformation (9, 10). The birefringence is about -0.055 for sodium light at room temperature.

The dielectric constants of single domain crystals for fields applied in the c and a directions have been measured by Mertz (10). The susceptibilities at room temperature are $\chi_a = 5000$ and $\chi_c = 300$ (where $\chi = \frac{\epsilon}{\epsilon_0} - 1$). Measurements of the dielectric constant as a function of frequency have indicated a relaxation commencing in the ceramic at about 10^8 cycles. (12,13)

In the perovskite structure of barium titanate, the barium ions are at the corners, oxygen ions at the face centers and titanium ions at the body center of the simple cubic unit cell. The spontaneous polarization is generally considered to be associated with the displacement of the titanium ions from the center of the original cube. Because of the relative simplicity of this structure, barium titanate is a ferroelectric material for which there is hope of an eventual detailed theoretical description. As von Hippel (14) has suggested, to explain the existence of a

spontaneous polarization, both ionic and covalent bonding must be invoked and a feedback effect introduced correlating the motions of the titanium and oxygen ions. Slater (15) has shown that the Lorentz field at the titanium ion, enhanced by the presence of the $(\frac{11}{22}0)$ and $(\frac{11}{22}1)$ oxygen ions, is more than enough to account for a spontaneous polarization. Devonshire (16) has advanced an "interaction" equation which is useful for correlating experimental parameters. Before a final molecular theory can be formulated, more detailed experimental information is needed.

After Matthias and von Hippel (17) discovered the existence of domains in the ferroelectric phases of barium titanate, Forsbergh (9) described the observed domain geometry in detail. 90° domains are regions of uniform polarization formed in the tetragonal phase by twinning on $\{101\}$ planes of the crystal. That the optical axis changes by 90° across a domain boundary can be verified with a quarter wave plate. "90° walls", as these twin planes will hereafter be called, are visible because of the distortion at the wall. Such domains are introduced into a crystal by the advance of thin wedges (17,9).

Recently it has been shown by optical means that there also exist domains formed by $\{100\}$ twin planes (18,19). Since there is normally no distortion at such a twin plane (180° wall) and a polar axis change of 180° can not be detected by either optical or x-ray techniques, the existence of these antiparallel domains was originally concluded by indirect evidence from distorted hysteresis loops (10,14).

The initial polarization curve of barium titanate, the dielectric non-linearity, hysteresis loops and their frequency dependence are to a large extent caused by the generation, motion, and interaction of domains. In contrast to the opaque ferromagnetic materials, where domain effects can only be studied at the surface by the Bitter technique, the transparent ferroelectrics allow an optical investigation throughout the volume by birefringence observations. In this way, static domain patterns as well as domain dynamics can be followed in all details and the electrical characteristics of the material interpreted by unambiguous optical evidence. This knowledge is needed for an understanding of the operation, possibilities and limitations of ferroelectric devices like transducers, memory devices and dielectric amplifiers. The present study on the dynamics of domain walls is a first installment to acquire this knowledge.

II. EXPERIMENTAL PROCEDURES

Preparation of Crystals

The crystals used in these experiments were grown from ternary melts following the method of Matthias et al. (7,8). By varying the composition of the melt and the heating cycle over a wide range, a variety of growth habits, crystal sizes and degrees of perfection could be obtained. By trial and error the "best" kind of crystal for the proposed research was established. Large crystals and "c" crystals, - that is, flat crystals with the polar axis perpendicular to the crystal plane, - have too many domains for simple visual experiments. In contrast, very thin, perfect "a" crystals - crystals for which the polar axis lies in the crystal plane, - prove ideal for visual experiments. The receipt finally used provided a maximum yield of these thin "a" crystals.

Fifty grams of BaCl_2 , twenty-five grams of BaCO_3 and five grams of TiO_3 , ground together in a mortar, were heated in an alundum crucible in one half hour to 1400°C , held at this peak temperature for one hour, and then cooled (in one hour to 1200°C , in five hours to 900°C). After dissolving the BaCl_2 flux in water, the single domain "a" crystals were selected by microscopic inspection. The crystals thus obtained are about ten microns thick and 400×400 microns² in area. While the large faces are $\{100\}$ planes, the edges may be $\langle 100 \rangle$ or $\langle 101 \rangle$ directions. We will call such crystals $[100]$ and $[101]$ crystals respectively. Although the small size causes experimental difficulties, the

simplicity of the domain patterns justifies the effort. Because of the thinness of the sample, most domain patterns varied only in two dimensions, that is, domain walls extended through the thickness of the crystal.

After heating above the Curie point, a perfect thin "a" crystal will almost always cool as a single domain "a" crystal. Two reasons for this behavior immediately suggest themselves. Either there is a slight memory built in during the crystal growth, or else, as in the magnetic case, the depolarizing field plays a part in domain formation. Since extraneous deposits or electrodes on crystal surfaces can sometimes determine the direction of the polar axis after cooling from above the Curie point, the domain habit of thin "a" crystals appears to be not entirely determined by built-in strain. On the other hand, the availability of free charge to neutralize the closing fields and the important effects of slight strains and imperfections on domain formation suggest that the depolarizing fields may not play as important a role in domain formation at the Curie point in a barium titanate ferroelectric as in ferromagnetic materials. Possibly both effects are present in greater or lesser degrees depending upon the conductivity and perfection of the crystals.

To provide electrodes, the crystal is laid flat on a microscope slide and, by using a micromanipulator, Dupont silver paint #4548 is spread along the glass and onto two opposite edges of the crystal. This is a difficult procedure and, undoubtedly, the resulting electrodes are not perfect. However, no effects attributable to poor electric contact were encountered, hence

the electrodes seemed adequate. Since the crystal electrodes are continued by the silver paint on the glass, wires can easily be attached to the paint well removed from the tiny crystal itself.

Microscopic Techniques

Because of the birefringence of barium titanate, the polarizing microscope is the ideal tool for a study of domain structure. Viewed along the polar axis, a domain acts as if in the cubic phase and appears black under crossed Nicols. Viewed perpendicular to the polar axis, as in the case of our "a" crystals, a domain will transmit light unless the light is polarized parallel to the "c" or "a" axis. In the latter conditions the domain is oriented at extinction.

Since the mechanical, electrical and optical axes are related, (cf. Appendix A), the extinction direction will be rotated, if the crystal is distorted electrically or mechanically. By observing the rotation of the extinction direction in an electric field, the uniformity of the field and the existence of strains in the crystal can be studied.

The optical magnification in these studies ranged up to 1100X.

Two tools were used for measuring wall displacements: a micrometer eyepiece, suitable for most observations, and microphotography, for very high magnifications or fast processes. For photography, a Lande camera proved invaluable as a descriptive recording device; a 16 mm Cine-Kodak movie camera with frame speeds up to 64 per second served for wall motion studies. Wall

movements down to one-half micron could thus be measured easily on a standard microfilm viewer.

A carbon arc lamp with a water cell for cooling provided a high intensity light source. It was found possible to achieve a sufficiently intense illumination, by very careful alignment of the optical system, for taking photographs with Super XX film at 1100X magnification and 64 frames per second with the Nicols crossed and the crystal axes oriented at 45° from extinction. For photographs with the axes near extinction, the magnification had to be decreased to 250X and the frame speed lowered to 16 frames per second. Though the Nicols need not be crossed for the observation of a 90° wall, internal scattering of light in the microscope for parallel Nicols proves disturbing. The exposure data given above represents the maximum speed and magnification at which readable films could be obtained.

For photographs of any kind it was found essential to have a prism and telescope arrangement above the ocular for final adjustments and visual observation of the crystal during filming.

Vibrations of the microscope stand were suppressed by foam rubber. A light tight adapter prevented direct contact between the microscope and the camera.

Electrical Instrumentation

A small furnace fitting the microscope stage allowed observations at temperatures up to 150°C .

To provide various types of electric fields, several power supplies were used. Short rectangular pulses of from 10 to 200

microseconds duration could be produced by the pulse generator of Fig. 1 a. For pulses $\frac{1}{4}$ to 3 microseconds long, the circuit shown in Fig. 1 b was employed. Observation and calibration of the pulse shape and height were made with the help of an oscilloscope connected across the crystal electrodes. The rise and decay time of the pulses proved negligible compared to the pulse length except for the $\frac{1}{4}$ microsecond pulses which were slightly bell-shaped. The width of such a pulse at 70% of its height was $\frac{1}{4}$ microsecond.

For rectangular pulses of the order of seconds or longer a toggle switch connecting to "B" batteries was employed (switching time $< 1/100$ second).

AC fields were provided by a standard low frequency generator ranging from 10^{-2} to 10^3 cps; by an audio oscillator covering the range from 20 to 20,000 cps; and by a bridge oscillator giving the selected frequencies - 30, 70, and 300 kcps. Wave forms and voltage amplitudes were measured on a scope.

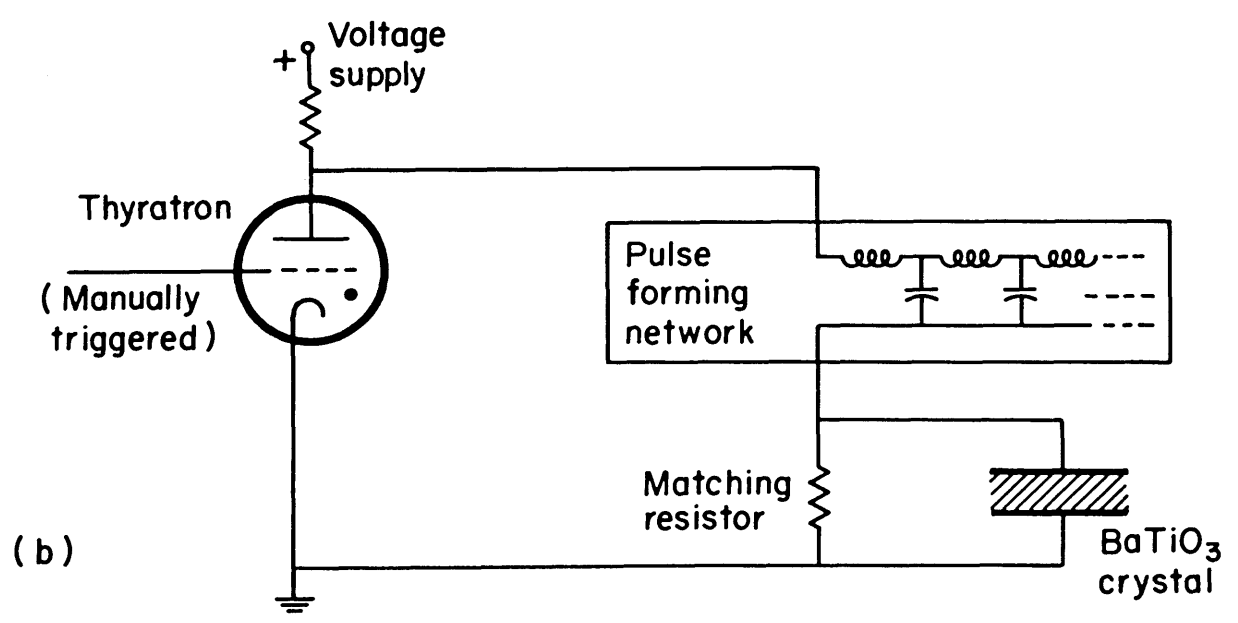
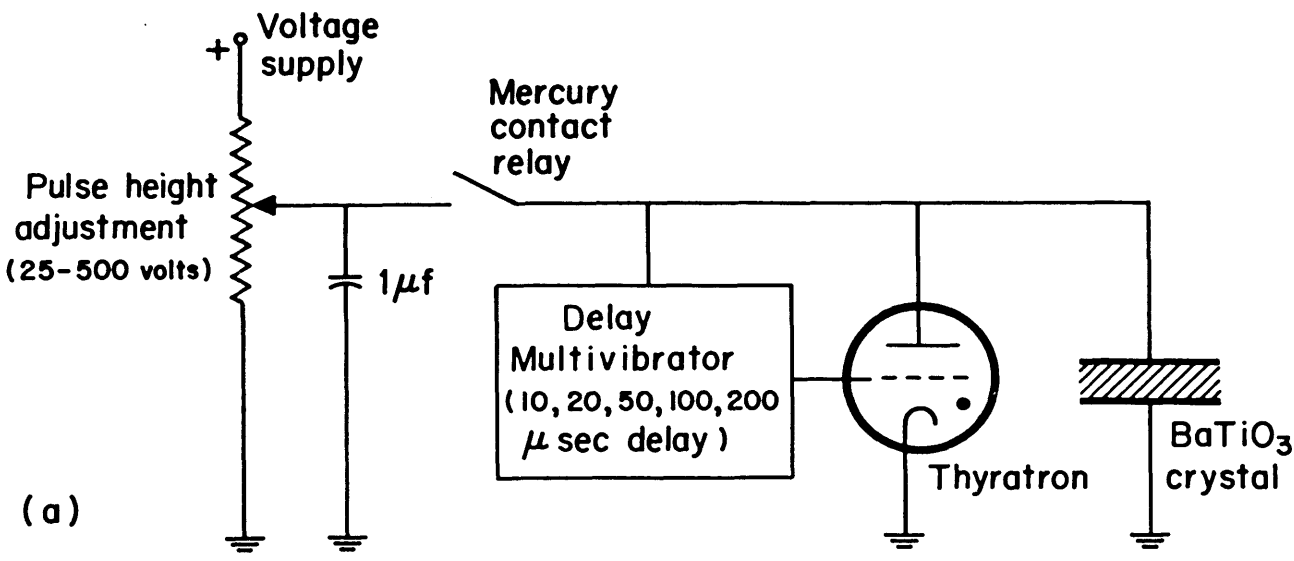


Fig. 1. Rectangular pulse generator circuits.

III. ANTIPARALLEL DOMAINS

An electric field across a barium titanate crystal tends to increase the total polarization in the field direction by four processes: the polarization in a single domain may rotate; the permanent moment may vary by additional displacement of the ions (induced moment); favorably oriented domains may grow at the expense of neighbors not so favorably oriented; and new domains may form. While all four effects will occur, we are concerned here with the last two preferentially.

In a "c" crystal or a [001] crystal with the polar axis parallel to the field, a field opposite to the polar axis will favor the creation and growth of antiparallel domains. However, since there is normally no observable distortion at 180° walls at magnifications up to 1100X, antiparallel domains in such crystals are not visible. Mertz first (18) made 180° domains visible by applying an electric field normal to the c axis of the crystal. The polar axes in adjacent antiparallel domains are rotated in opposite directions by the field and therefore differ in their extinction directions (Fig. 2). For an optical study of the dynamic behavior of 180° walls, thin "a" crystals with {101} edges are therefore uniquely suited. One component of the field makes the domains visible and the other component forces the domains to grow. If not very large fields are applied, the additional formation of 90° domains can be avoided. Fig. 3 shows such a [101] crystal with its antiparallel domains: the domains of one polarity are in extinction (black) and those of the opposite polarity transmit light.

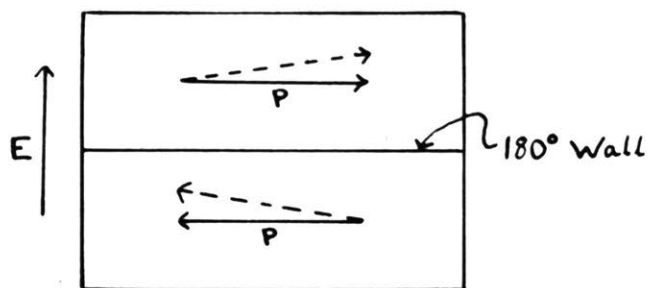


Fig. 2. Rotation of polar axes near a 180° wall in a field perpendicular to the wall.

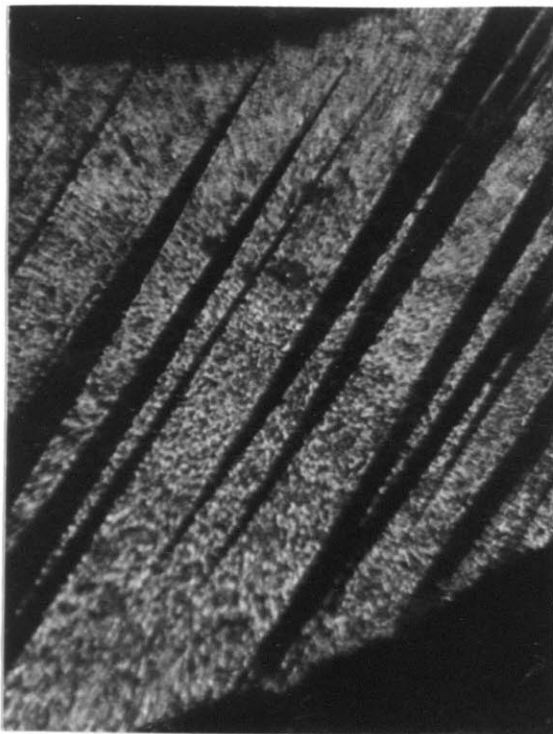
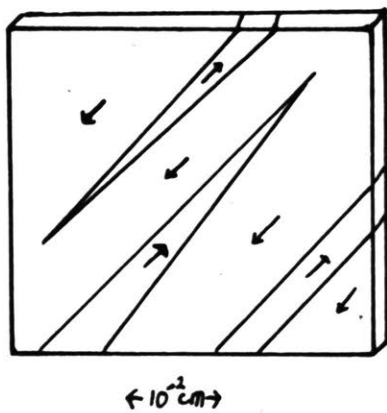


Fig. 3. 180° domains in a [101] crystal.

One can observe visually that a transition region of about $\frac{1}{2}$ micron width at the wall does not rotate in the field and that a very slight optical distortion extends as far as 5 microns into the crystal.

For the subsequent section the field strength, E , quoted is applied to the $[101]$ crystal; the field component inducing growth of domains is only $E/\sqrt{2}$. A field strength is designated as negative when opposite to the initial polarization of the crystal.

Nucleation and Initial Motion

In studying the growth of antiparallel domains, we have to answer several questions: how do antiparallel domains form?; how fast do the domains grow in the c direction?; and how do they widen perpendicular to the polar axis in a given field?

As a starting experiment short rectangular pulses were applied to a single domain crystal.

A negative pulse of 7.4 kv/cm (length 200 microseconds or shorter) applied to a single domain crystal at extinction causes normally nothing but a barely perceptible flash of light no matter how many such pulses are applied in succession. Reversing the field direction shows nothing different. We cannot say for sure that no domains were introduced by the pulses, but certainly no permanent domains were formed. With continuous pulsing, occasionally some thin ($\frac{1}{2}$ to 5 microns at the widest part) spikes appear, extending from one edge nearly across the crystal (0.05 cm); they remain visible for as long as a second after pulsing. For as

many as fifty subsequent pulses these same wedges have been observed; they do not appear to grow. If the direction of the field is now reversed, the first pulse will reveal for about a second the same wedges shortened to about 0.01 cm.

No wedges were ever observed to form for pulses shorter than 10 microseconds in fields up to 11 kv/cm, or in fields below 7 kv/cm for pulses shorter than 200 microseconds. (A spike thinner than $\frac{1}{2}$ micron would not be visible.)

Additional information was obtained by performing the inverse to the preceding experiment. A few large (20 microns wide and 500 microns long) antiparallel domains were introduced into the crystal by a low negative DC field. These wedges, left undisturbed, will remain in the crystal for 24 hours or longer. Short positive pulses ($E = 7.4$ kv/cm) spaced several seconds apart were applied to remove the wedges and the number of pulses required recorded as a function of pulse length (Fig. 4). As each pulse is applied, the domains still present become visible for about a second. If the pulse rate is increased, more pulses are required for the removal of the wedges.

When pulses of 10 microseconds or longer are used, some domains are removed entirely by the first pulse; a bright region left behind fades out in about a second. For pulses shorter than one microsecond, each pulse narrows the domains significantly and the wedge tip retreats a little.

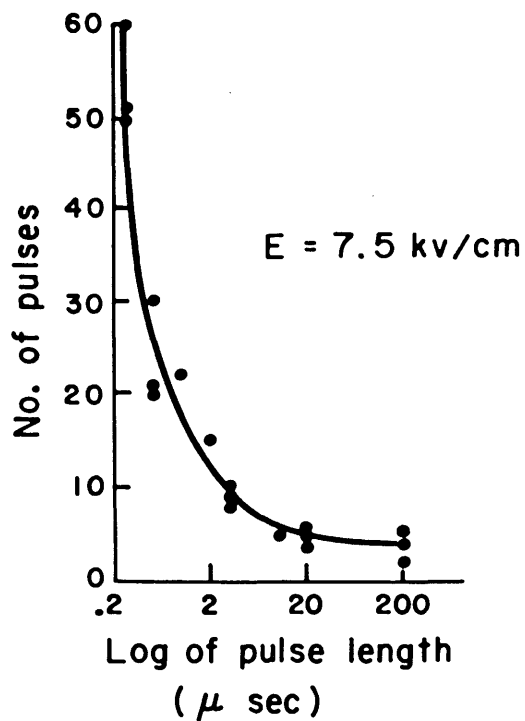


Fig. 4. Number of pulses required to remove 180° domains as a function of pulse length.

Discussion

Two tentative conclusions can be drawn from these experiments. (1) The formation of an antiparallel domain begins as a spike at the edge of the crystal; it extends along the polar axis with a velocity between 5×10^3 and 5×10^4 cm/sec. (2) Space charge effects appear associated with the stabilization of the wedges; their relaxation time in our crystals is of the order of a second.

This second conclusion, based on the visible after-effects of pulses, requires a closer examination. If a 180° domain is wedge-shaped with a wedge angle θ , the saturation polarization, P_s , produces a large electric field, $\sim \frac{P_s}{\epsilon_0} \sin \theta \sim 10^5 \sin \theta$ kv/cm, at the walls, caused by the free ends of the dipole chains. Such a field should create a large lattice distortion near the 180° wall, but quasi-stationary domains with a wedge angle of 20° or more do not show such distortions. This suggests that a compensating electric charge accumulates and neutralizes the ends of the dipole chains.

Since the initial wedge velocity is so high, and the relaxation time of the free charge according to the fading of the bright region is of the order of a second, the space charge is not able to follow the domain wall motion during the initial propagation of a 180° domain or during the motion caused by a pulse of 200 microseconds or less. However, thin domains without appreciable wedge angle might be nucleated and removed by short pulses. As soon as compensating charge can accumulate on domain walls, domains are stabilized.

This concept receives support from the experiment which measures the number of pulses required to remove domains (Fig. 4). The curve found can be expressed by the equation

$$N = 2.8 \ln t_0/t \quad (1)$$

where t is the pulse length and t_0 equals 0.15 microseconds. This increase in the required number of pulses with decreasing time becomes understandable if the domain wall velocity decreases as it leaves its space charge behind. Many short pulses spaced by intervals of several seconds allow the space charge to catch up and prove therefore more effective in removing domains than a few long pulses, as long as the pulse length is short in comparison to the time constant of the space charge motion.

That an antiparallel domain can be removed by several positive pulses of the order of microseconds, but not observably increased by a large number of corresponding negative pulses, can be explained by the fact that the electrostatic energy of the closing field is reduced when a domain diminishes in size.

These experiments are in line with the concept of von Hippel (20) that the conductivity of BaTiO_3 crystals is of great importance for the dynamics of the domain formation, and with observations by Mitsui and Furuichi (21) on the effect of charges on the domains in Rochelle salt crystals.

Reversal of the Saturation Polarization by Antiparallel Domains

The manner in which spikes widen and lengthen in a negative DC field until the crystal is completely polarized in the reverse

direction is illustrated schematically in Fig. 5. The domains are wedge-shaped at every stage of growth. The last domains to leave are wide wedges at the edges of the crystal; they are often difficult to remove completely even with a high field.

To study these slow processes and avoid the formation of 90° wedges, a negative field is applied gradually to a single domain crystal, reaching its peak field strength, E , in about $\frac{1}{2}$ second. Typical thin spikes starting from both directions extend across the crystal before E is reached. These spikes tend to nucleate at identical places at the edge of the crystal when the experiment is repeated. The number of such spikes, which depends on E as well as on the time derivative of the field, is plotted against E in Fig. 6. The times required to reach approximately 50% (a) or 90% (b) reversal is shown as a function of the peak field strength in Fig. 7, (the areas of opposite polarity were estimated visually). Since $1/t$ is related to the velocity of reversal and is easier to discuss, this parameter has also been plotted in Fig. 7 in its dependence on E .

The characteristics show that a minimum field strength of about 2 kv/cm is required for the nucleation of the wedges. In fields smaller than 2 kv/cm, no wedges are formed during the observation period of 24 hours. For E smaller than about 2.4 kv/cm, the wedges do not grow for times as long as 12 hours. Therefore, for all practical purposes, in our $[101]$ crystals the limiting field, E_c , for nucleation and growth of antiparallel domains is nearly the same. The growth velocity is slowed down

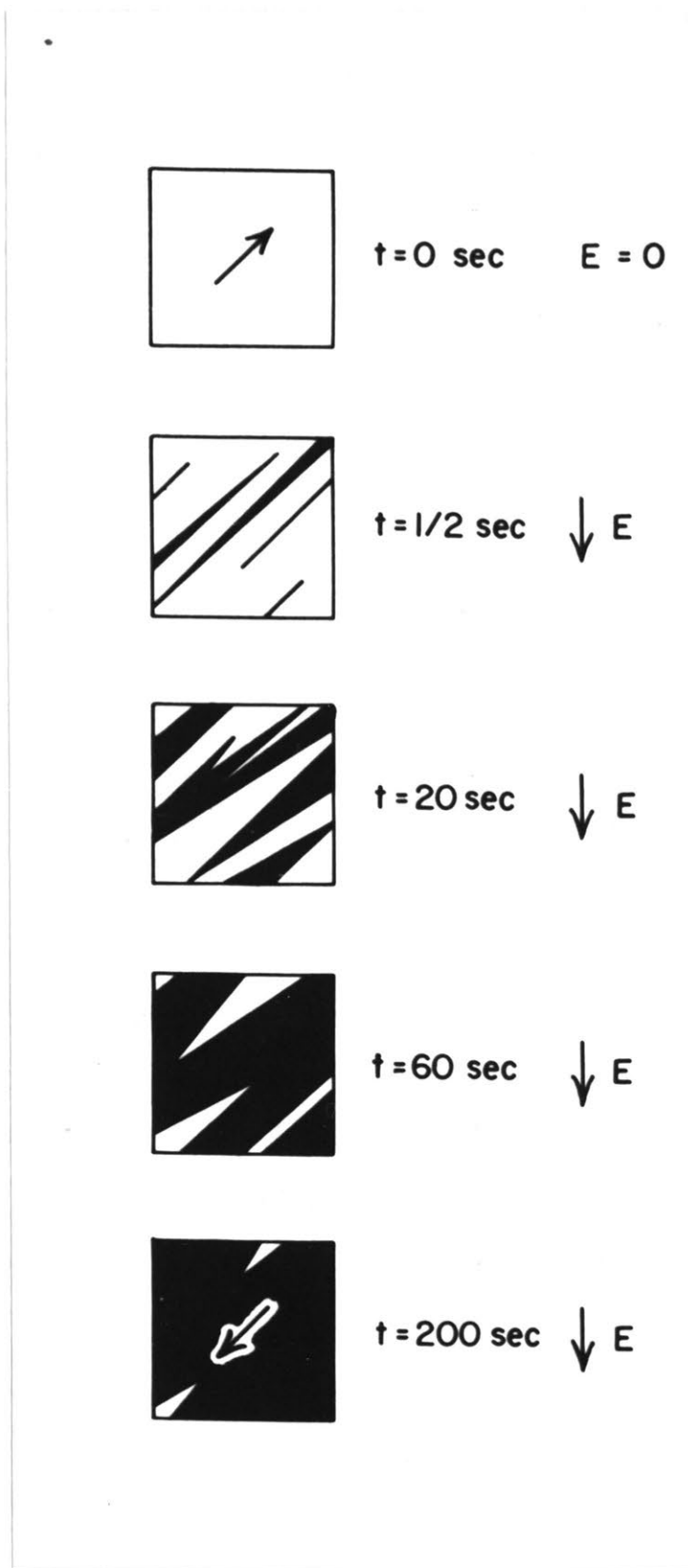


Fig. 5. Schematic diagram of 180° domain switching process in $[10]$ crystals.

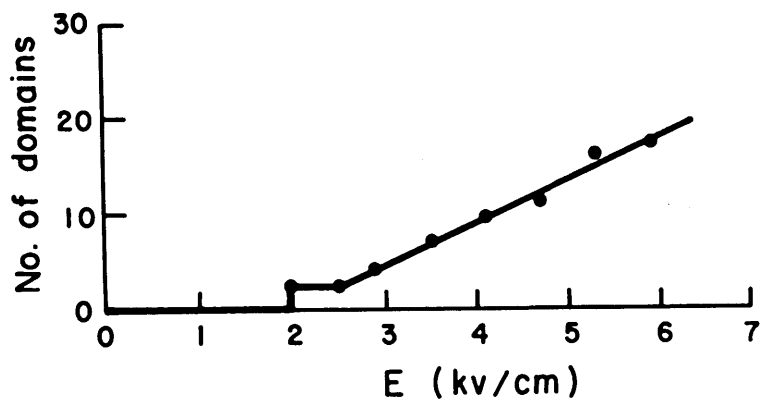


Fig. 6. Number of 180° domains nucleated in a DC field as a function of field strength.

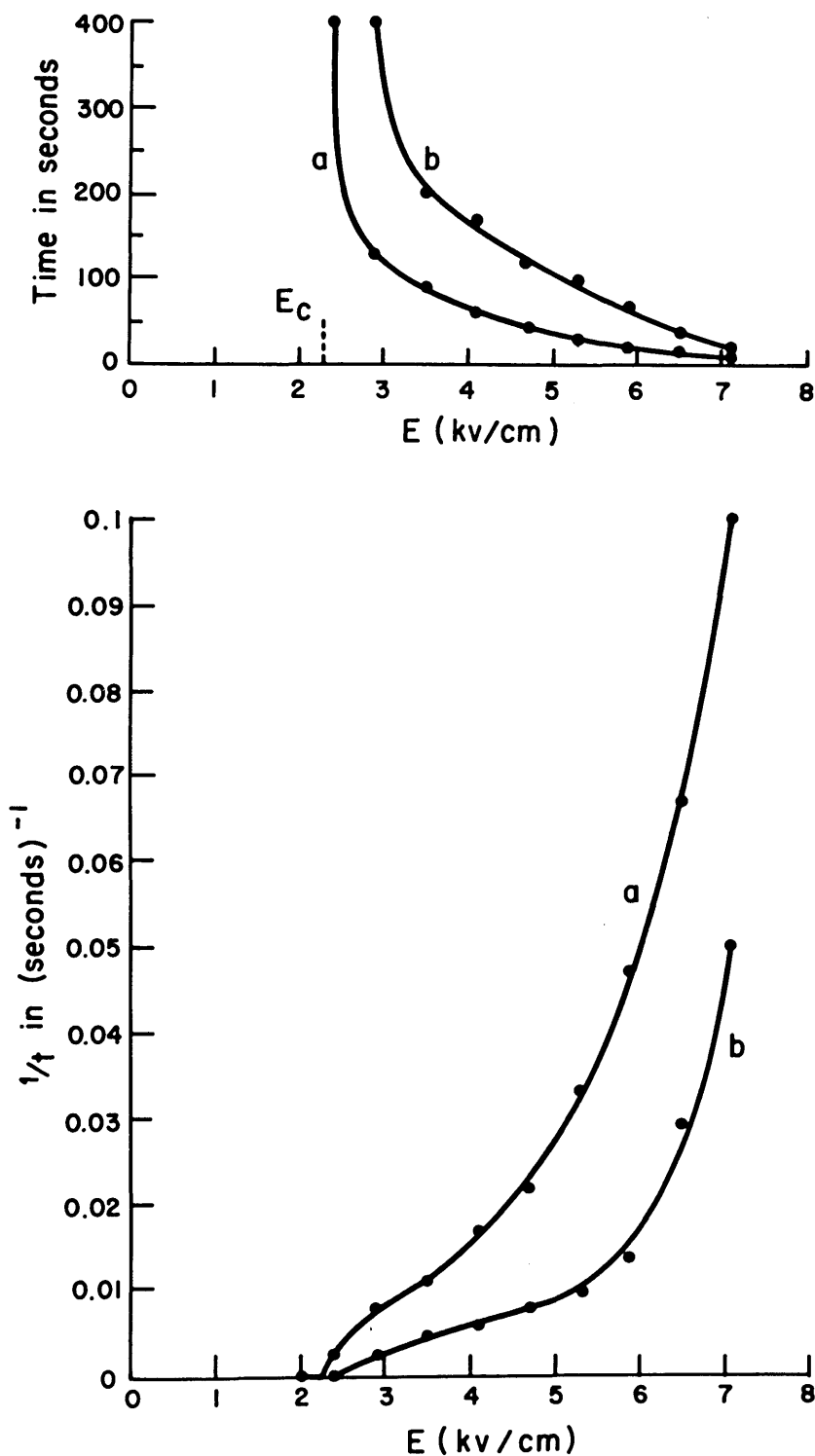


Fig. 7. Time required for 180° domains to reverse the polarization of a $[101]$ crystal a) by 50% and b) by 90%. Both the time and $1/\text{time}$ are shown as a function of DC field strength.

appreciably in the last stages of reversal. This effect is related to the widening of the wedges; the wedge angles increase to nearly 30° . Differently expressed, a large field and a long time are required to saturate or "prepolarize" a crystal, as has been observed already by electric measurements (10,14).

The shape of the curves (Fig. 7) leads again to the interpretation that the advance of spikes, initially fast, is slowed down as the electrostatic energy of the depolarizing field increases and that growth continues as a neutralizing charge accumulates on the domain walls. Therefore, we have to distinguish between two processes: the propagation of a spike with no charge compensation and the growth of a wedge with charge compensation. Speed and size in both cases increases with the field, and the time needed for 50% saturation will include both effects, while the time required to reverse the polarization from 50% to 90% should primarily reflect the growth rate of wedges with charge compensation. The number of walls present at 50% saturation is nearly constant for the range $3 < E < 6$ kv/cm and in this range the growth velocity of wide wedges increases about linearly with $E - E_c$. Beyond 6 kv/cm, the initial fast mechanism becomes more predominant, the slope of $1/t$ vs. E increases and if E could be made large enough a crystal might be switched to opposite polarity in a very short time.

Temperature increase appears not significantly to change the times of reversal. However, since 90° wedges appear in great numbers at elevated temperatures and hamper the motion of 180° domains, no great significance can be attached to these results.

If one breathes on the crystal the 180° domains move faster. Also a small photo effect seemed to exist: when the arc lamp was turned off, switching seemed to take a slightly longer time. Both effects are consistent with the idea that the conductivity of the crystals is of importance and that we have to consider surface as well as volume conductivity.

The major inconvenience for experiments on 180° domains is the appearance of 90° domains which cannot be avoided in all [101] crystals. While the results reported are common to the crystals in which we studied 180° domains, the average width and number of 180° domains seemed to vary from crystal to crystal. Since the imperfections and conductivity will vary from sample to sample, this is not astonishing. In a crystal in which the 180° domains stay thin over long times, implying a low conductivity, a restoring force seemed to act on the slow 180° wedges. After the DC field was removed, the wedges retreat somewhat. We may here view the restoring force of the depolarizing field.

Dielectric Measurements on 180° Walls

Since the walls are not simple linear oscillators, AC measurements are not an unambiguous tool for the study of domain dynamics, but they give important qualitative information. Fig. 8 a shows the "susceptibility" and loss tangent at high field strengths as a function of frequency for a large "c" crystal. The result that the wall motion damps out at around 10^4 cps is consistent with our optical results. Measurements on the tiny "a" crystals used for visual observations of wall motion proved difficult because the capacitance

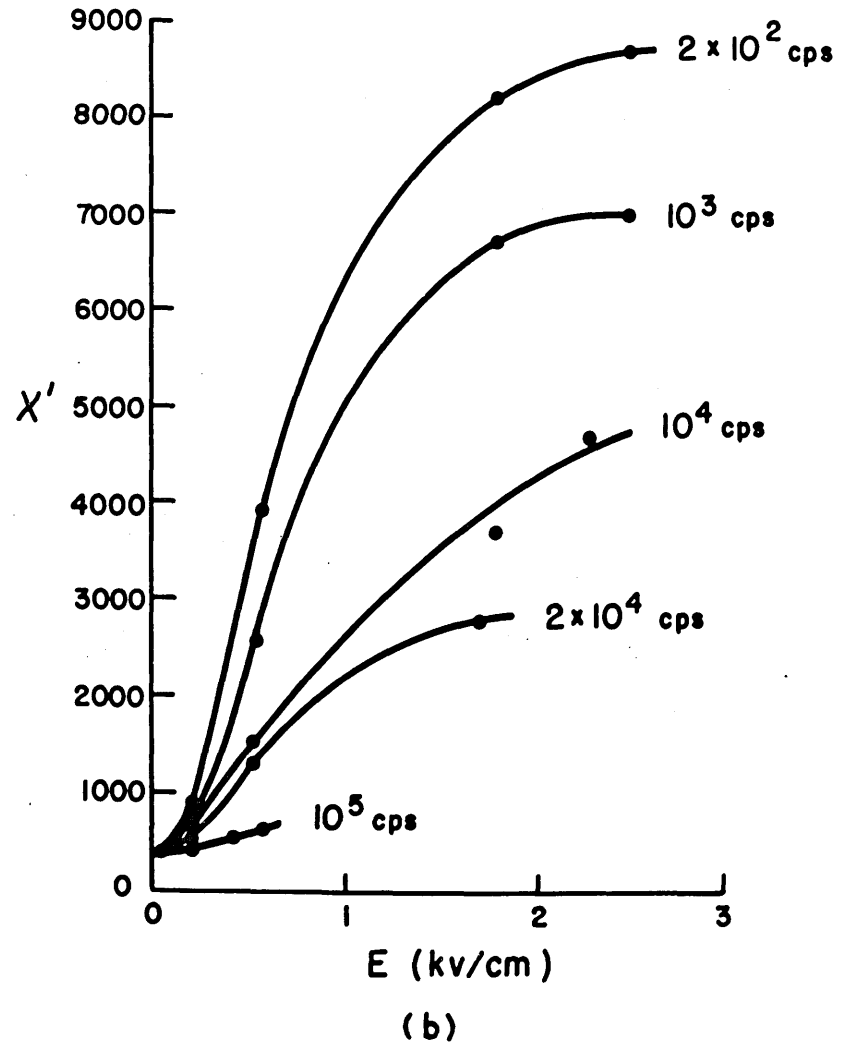
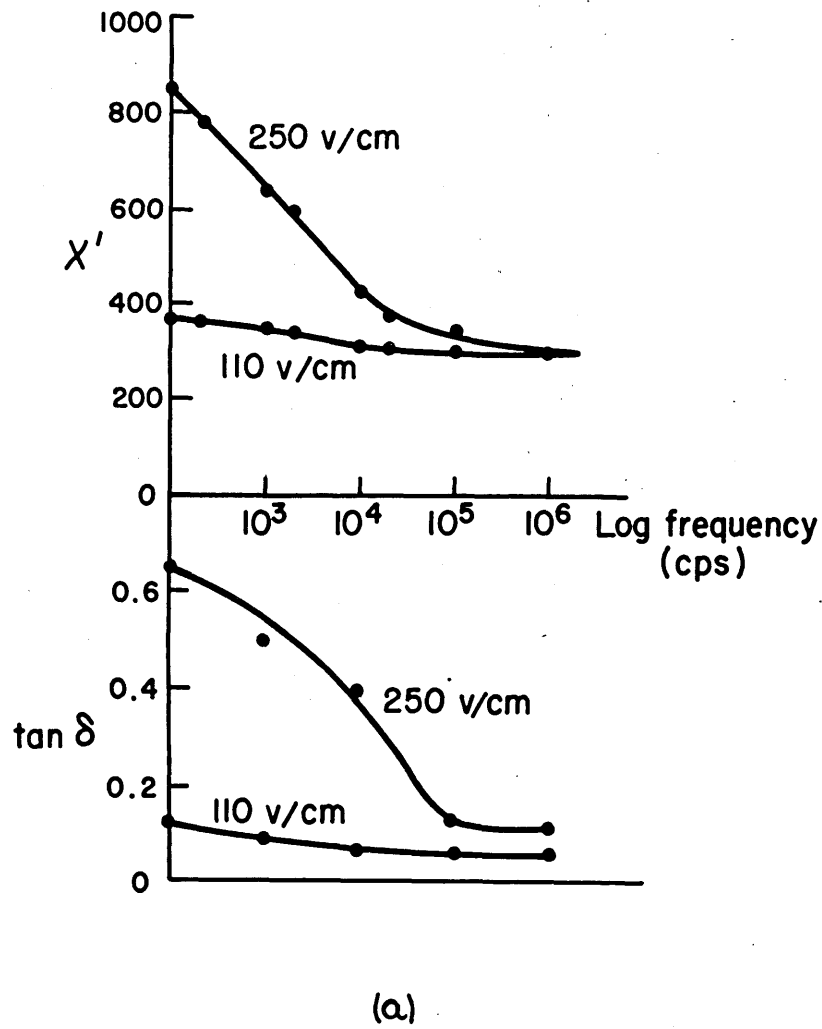


Fig. 8. Dependence of susceptibility and $\tan \delta$ on field strength and frequency; (a) "c" crystal, and (b) [001] "a" crystal.

was only of the order of tenths of micromicrofarads and the readings, especially of $\tan \delta$, fluctuated widely. Fig. 8 b gives some measurements of χ' for such a [001] crystal, mounted with the c axis parallel to the field. In this case, χ' is plotted against field strength with frequency as a parameter.

In both cases χ' approaches about 300 for low fields. The critical field for domain motion for the [001] crystals appears to be somewhat lower than observed visually for a [101] crystal, even when the different geometry is taken into account. This might imply that very thin and therefore invisible spikes move at low fields. The measurements show that domains move at 10^4 cps corresponding to a pulse time of about 50 microseconds. That χ' increases rapidly with decreasing frequency and reaches a maximum at lower fields gives electrical evidence of the slow switching process. Hyde in this laboratory (22) found by tracing hysteresis loops that the slope $\frac{\Delta P}{\Delta E}$ continues to increase for frequencies as low as 10^{-1} cps. This would be expected from our domain observations with DC fields.

Summary for 180° Domains

The results obtained thus far for the growth of 180° domains in a [101] crystal might be summarized as follows. If the field strength is larger than a critical field, E_c , thin spikes are nucleated, probably at imperfections, and move across the crystal with a high velocity. The spikes slow down as they broaden into wedges and await the accumulation of compensating charge as they widen and eventually merge to saturate the crystal. The total

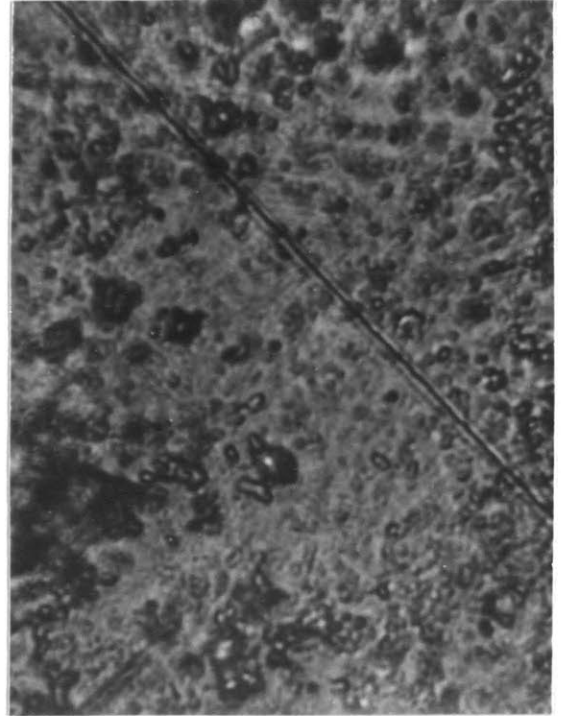
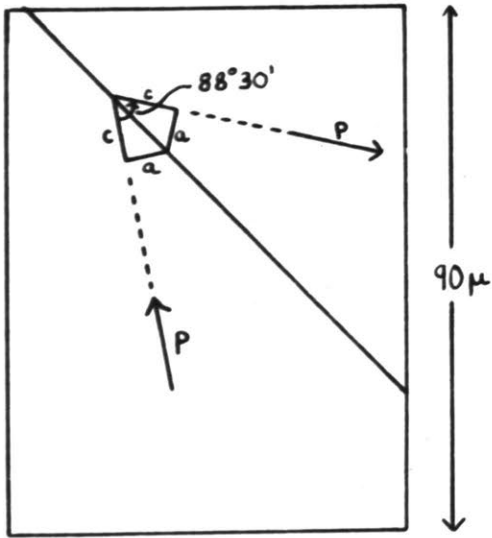
switching time is of the order of seconds for fields below 10 kv/cm. The critical field for growth in our crystals is nearly the same as the critical field for nucleation.

A more detailed model for 180° walls will be given later.

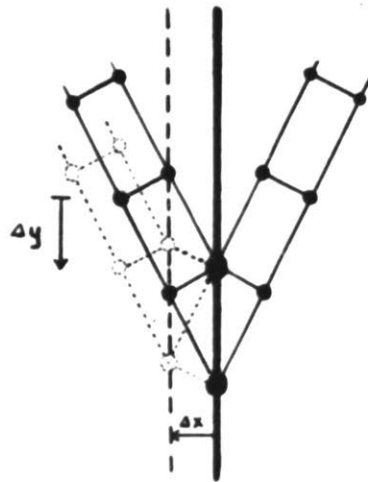
IV. 90° DOMAINS

A 90° wall is a $\{101\}$ twin plane and, in contrast to 180° walls, readily visible by transmitted light as a dark line approximately 0.4 microns thick. (Fig. 9 a) The ghosts at the edges of the line are caused by optical diffraction. They also appear at the edges of a crystal at high magnification. The optical axis of the domains adjacent to the 90° wall stand at an angle of 45°45' to the wall at room temperature. This is the angle corresponding to the ratio of the a to c edges in a unit cell, $\tan^{-1} a/c$. (Fig. 9 a) A 90° wall should accurately be called an 88°30' wall, a concept of importance for the study of wall dynamics. Because of the 1°30' difference in orientation between the crystal axes across a 90° twin plane, the displacement of a wall by Δx implies slip of one domain with respect to its neighbor by $\Delta y \sim \frac{\Delta x}{20}$, (Fig. 9 b). Naturally, pressure exerted on a crystal, for example by a needle, can both introduce and move 90° domain walls.

To study 90° domains without interference by 180° domains, we selected a $[100]$ crystal with the polar axis perpendicular to the electrodes. A good crystal of this kind is initially a single domain crystal. A DC field exercises in such a crystal no force tending to create antiparallel domains, but a large torque tending to rotate the polar axis by 90°. If the field is increased slowly, at a critical field strength, E_c , 90° wedges are nucleated (Fig. 10a). The wedges, 2 to 10 microns wide, extend across the crystal (about 0.05 cm) in less than 1/100 sec. Fig. 10c shows, in an unusually uniform pattern, the wedge structure in detail. If the field is

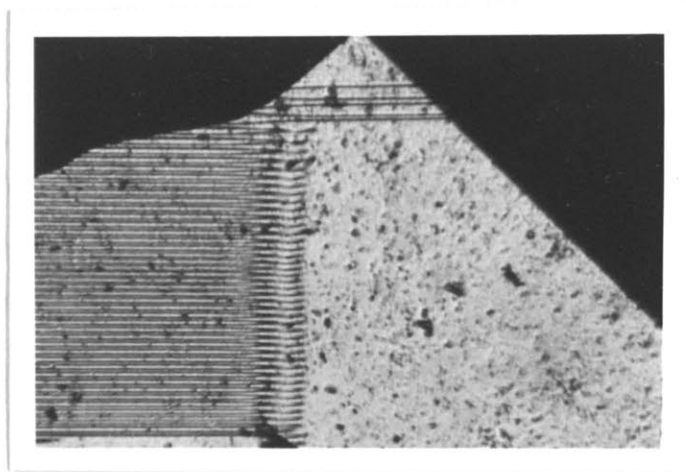
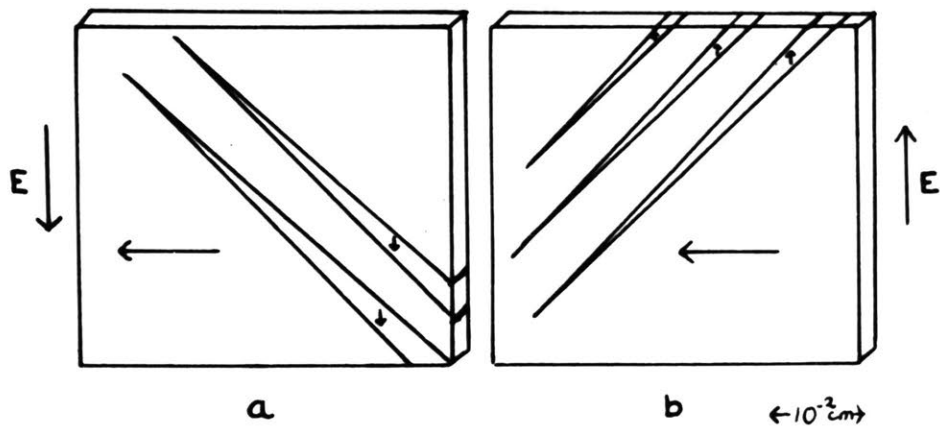


(a)



(b)

Fig. 9. a) 90° wall showing $1^\circ 30'$ distortion.
b) 90° wall motion Δx showing corresponding slip Δy (exaggerated).



c

Fig. 10. 90° wedges. a) Nucleation in a $[100]$ crystal for a positive field, b) nucleation for a negative field, and c) some 90° wedges.

removed, the stresses caused in the crystal by the presence of 90° domains may frequently force the wedges out of the crystal. They shrink slowly at first and then disappear suddenly. However, we observed several times, after the wedge had disappeared, a slight distortion about one micron wide and 10 microns long fading away in the direction in which the wedge had disappeared. A close study of Fig. 10 c shows that near the wedge tips the walls are blurred.

In a field of opposite polarity (Fig. 10b), 90° wedges will enter from the opposite side of the crystal. Such a polarity dependence for 90° wedges, (in each case they start from the cathode), was almost invariably observed in all crystals. However, there were exceptions, particularly at higher temperatures.

For reasons which will become apparent later, a crystal (called crystal "A") was chosen for the following experiments, because 90° wedges were always forced out of it by stresses when the field was removed. The field required to maintain wedges in the crystal was about 1 kv/cm; it serves as a measure of the magnitude of the mechanical stresses involved. The critical field strength, E_c , of crystal "A" is plotted against temperature in Fig. 11 for static fields. The similarity of the E_c vs. T characteristic with that of the spontaneous polarization or the strain of a single domain crystal as a function of temperature (10) suggests that these quantities are related.

Nucleation of 90° Domains

To determine the initial growth of 90° wedges as a function of time and field strength, a square pulse was applied to the

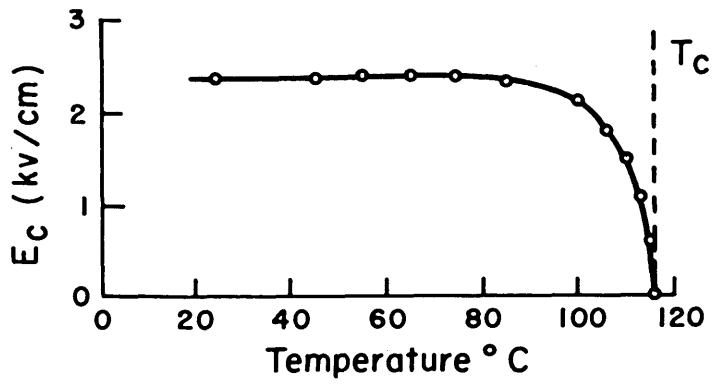


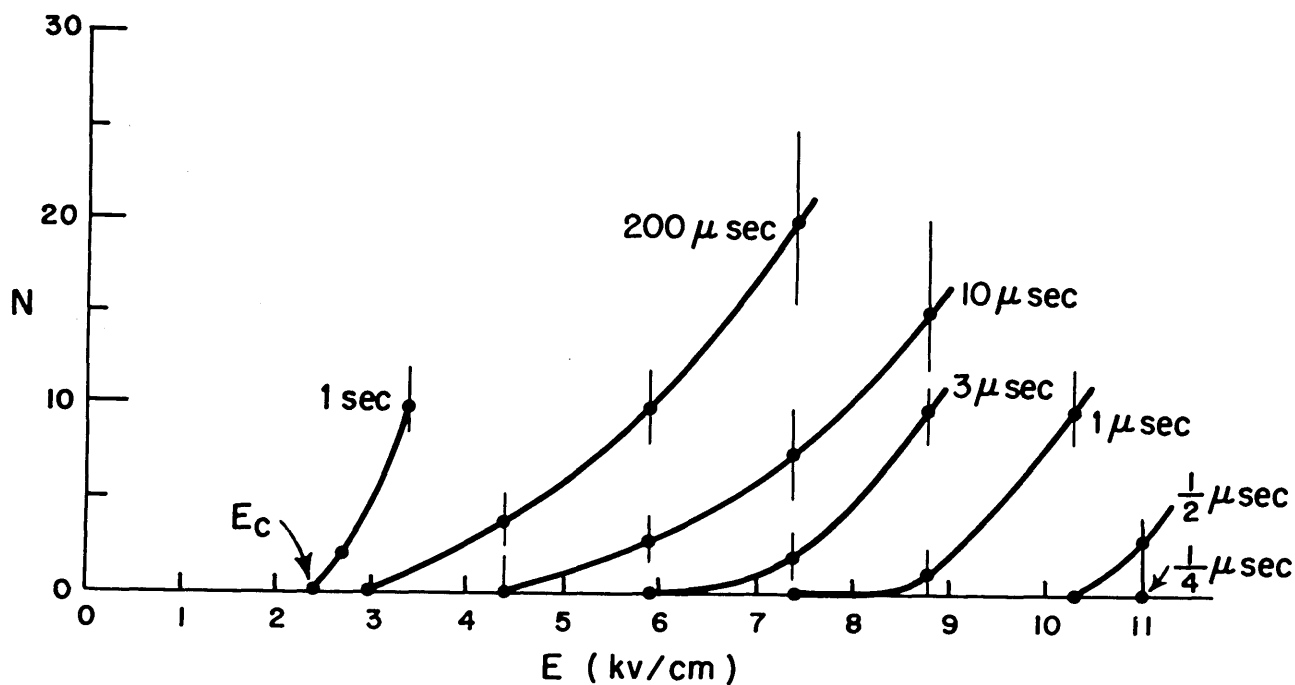
Fig. 11. Critical field for 90° wedge nucleation as a function of temperature.

single domain crystal "A" and the number of wedges in the crystal immediately afterwards recorded. After a few minutes of rest, strain had forced the domains out and restored the single domain crystal. The number of wedges was measured as a function of pulse height, E , and pulse time, t , (Fig. 12). Each measurement at a given E and t was repeated several times with very little scatter; the estimated accuracy is indicated.

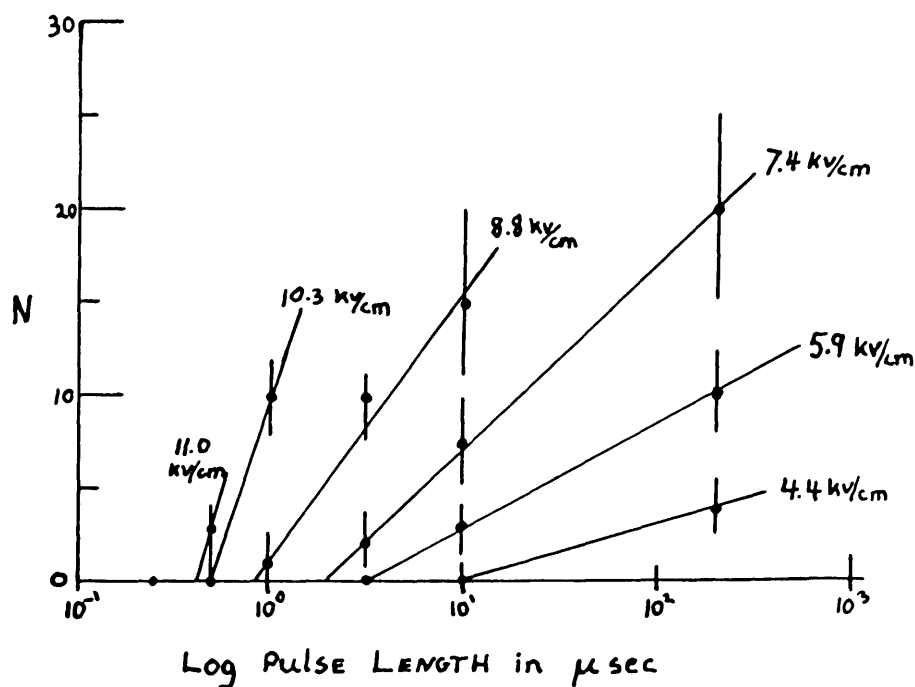
No wedges were ever observed for $\frac{1}{2}$ microsecond pulses and E smaller than 11 kv/cm; for pulse times longer than one microsecond, every domain observed extended across the crystal; for times shorter than one microsecond, some wedges did not reach across the crystal. Pulses longer than 10 microseconds widen the wedges a little after they have traversed the crystal. However, no wedges were wider than 20 microns for pulses of 200 microseconds or less. The expansion normal to the wedge axis proceeds with a velocity of about 100 cm/sec at 7.4 kv/cm.

With increasing temperature the fluctuation in the number of domains formed increased to complete randomness. However, at temperatures near the Curie point, the nucleation of wedges, as far as could be discovered, appeared reduced.

Fig. 12 shows that N increases with E and t . It is significant that there exists a threshold pulse length, t_0 , for a given field strength below which no wedges are formed. In Fig. 13, $(t_0)^{-\frac{1}{2}}$ is plotted against E ; it appears that $t_0(E-E_c)^2$ is about a constant for low fields. Also in Fig. 13 the log of the minimum pulse length is plotted against $1/E$. This curve fits



a



b

Fig. 12. Number, N , of 90° wedges nucleated by a square pulse, a) as a function of pulse height and b) as a function of pulse length.

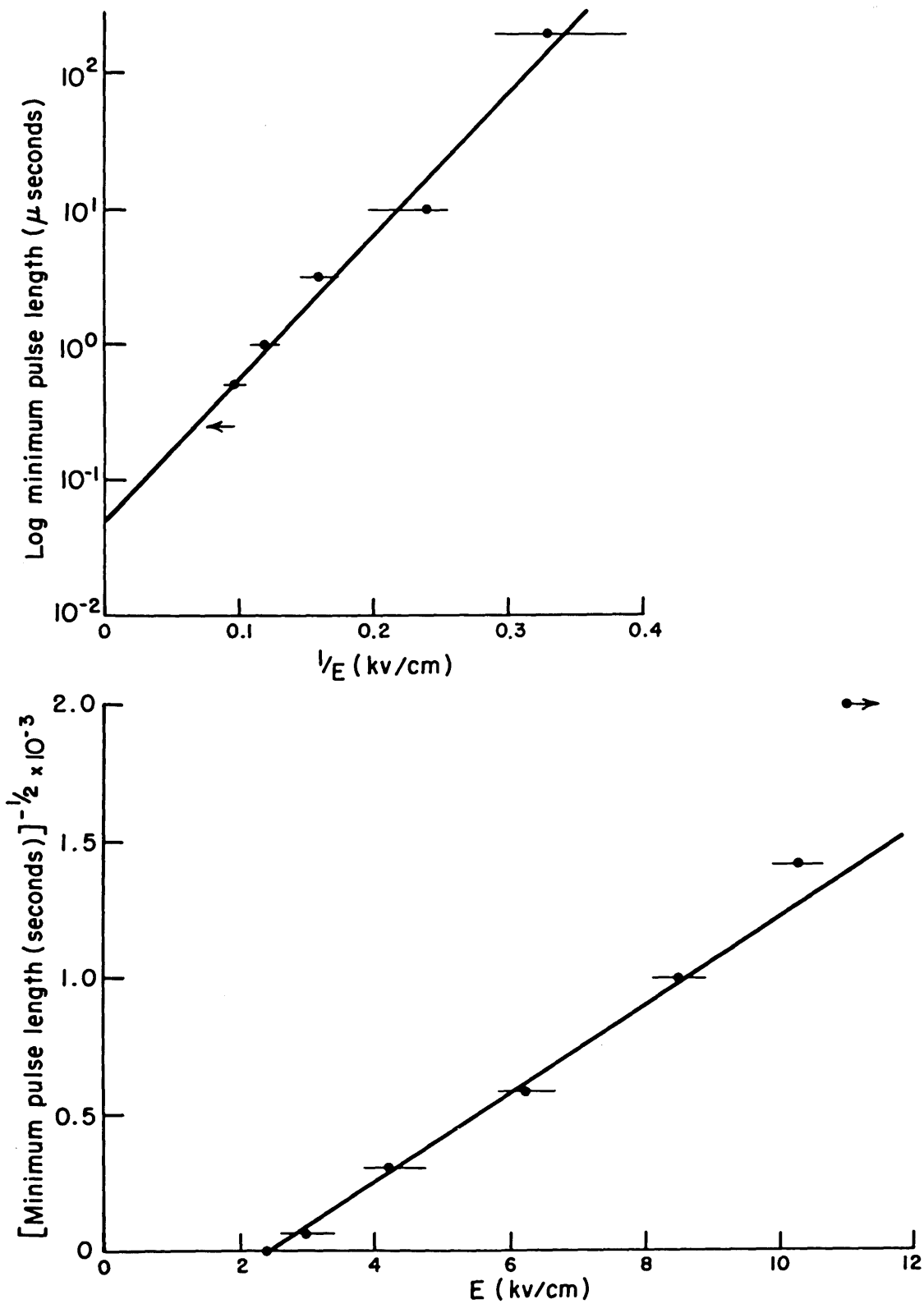


Fig. 13. Minimum pulse length, t_0 , for nucleation of 90° wedges as a function of pulse height, E.

best at high fields; that is, here

$$t_0 = t_s e^{\frac{B}{E}} \quad (2)$$

with $B = 25$ kv/cm and $t_s = 0.05$ microseconds.

When N is plotted against the log of t , (Fig. 12) it proves in a first approximation to be proportional to \ln/t_0 , hence

$$N = C \ln t/t_0 \quad (3)$$

at a given E , with C and t_0 dependent on E . Within the accuracy of the measurements,

$$C = C_0 e^{\gamma E} \quad (4)$$

where $C_0 = 0.28$ and $\gamma = 0.36 \times 10^{-5} \text{ (v/m)}^{-1}$. Therefore to a first approximation,

$$N = 0.28 e^{\gamma E} \ln t/t_0 \quad (5)$$

and

$$\frac{dN}{dt} = \frac{0.28 e^{\gamma E}}{t} \quad (6)$$

Thus the nucleation rate increases exponentially with E and decreases with $1/t$.

Both results appear not unreasonable. The time dependence must be visualized from the standpoint that as the domains form and grow, less material is available for the growth of new domains.

In summary, if a DC field greater than E_c is applied to crystal "A", 90° wedges are nucleated and travel across the crystal

with a high velocity. Both processes are accelerated by higher fields. There is a critical field for nucleation for a given time interval. The nucleation rate goes through a maximum value at constant field strength as a function of time.

If a 60 cps AC field is applied to crystal "A", domains are nucleated at about 2 rms kv/cm; in a high frequency field (300 kcps), the critical field for nucleation increases, as one would expect. However, before the threshold field is reached, a crystal may be heated by dielectric losses above the Curie temperature. The field required to heat our "A" crystal through the Curie point was about 5 rms kv/cm at 300 kcps. This heating effect is especially significant for a crystal without domains of any kind; we have not observed it under corresponding conditions in [101] crystals. The large internal friction accompanying the rotation of the dipoles and the corresponding shear of the lattice is thus demonstrated.

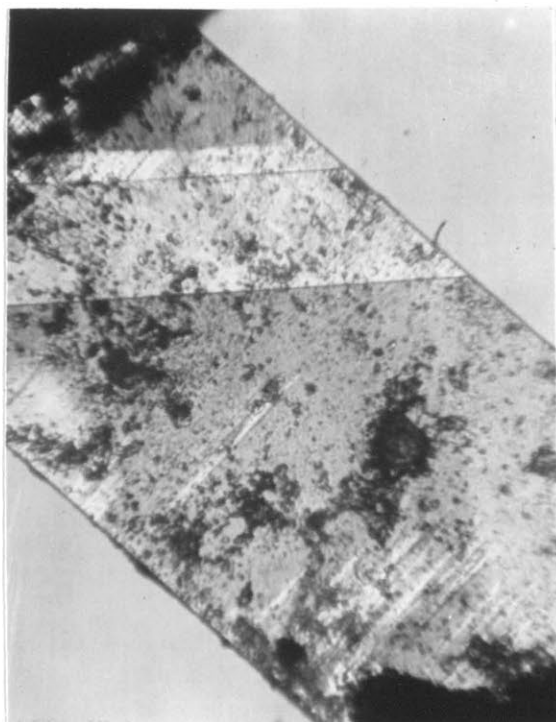
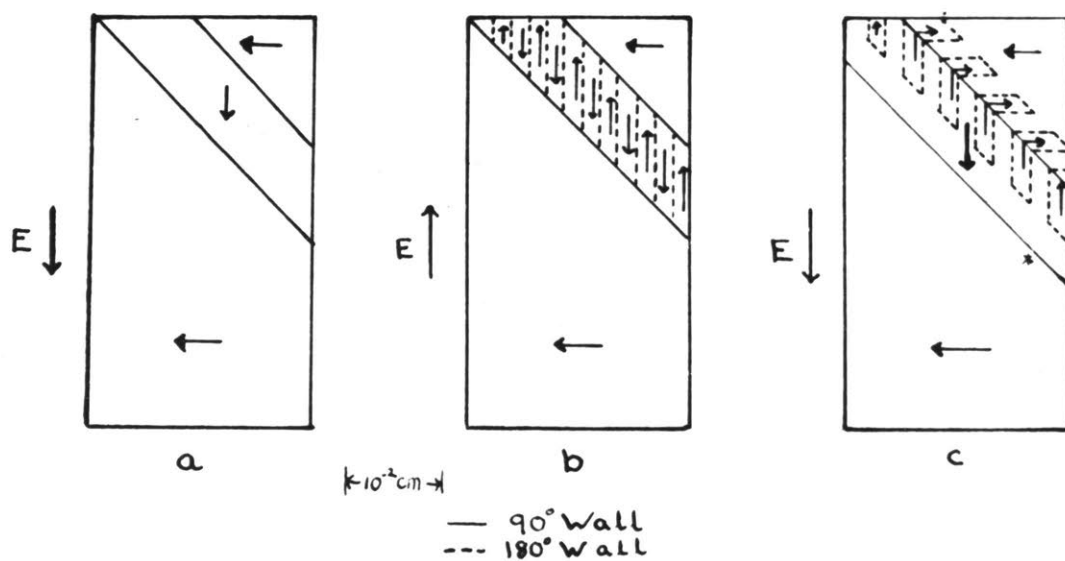
90° Wall Motion

After 90° wedges have been introduced into a crystal, domain growth can be described in terms of wall motion. Once a wedge has grown across a crystal, the two now parallel walls separate and move sideways with decreasing velocity and some irregularity until they come to a stop. In crystal "A", wall motion normal to a wall for a given field strength was very small. Even if the field is large enough to polarize the whole crystal in the field direction, removing the field will show domains forming to restore the crystal to its initial polarization. We conclude that crystal "A" has a built-in strain.

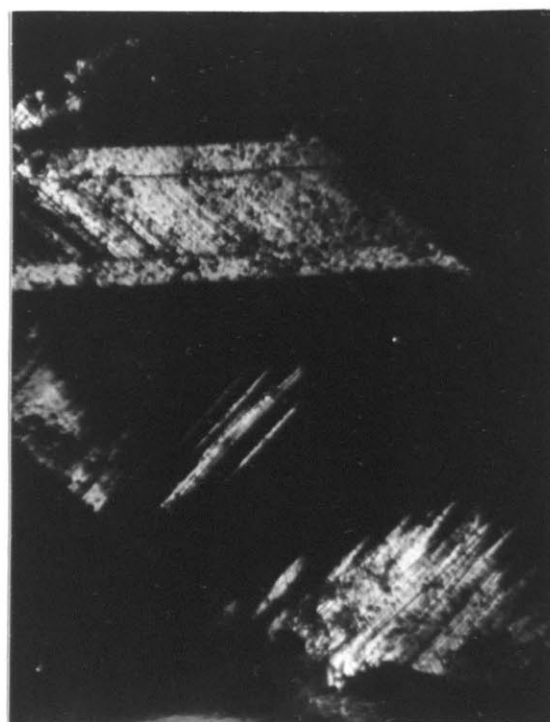
A second [100] crystal, "B", was studied, for which the strain effects proved appreciably smaller. A comparison of the rotation of the optical axes (Section VI) shows that in crystal "B" the rotation was larger for a given field than in crystal "A". As we would expect, when rotation is easier, the critical field strength, E_c , for the nucleation of wedges is higher; for crystal "B" it was about 6 kv/cm. After the walls became parallel, not only were much larger displacements obtained for a given field strength than in crystal "A", but in "B" wall motion occurred for field strengths of the order of several tenths of a kv/cm instead of several tenths in addition to a biasing field of one kv/cm. Removal of the DC field allowed the walls to retreat slightly but the domain usually did not leave crystal "B". However, if a small AC field was applied, the two walls drifted together and disappeared.

A DC field applied to crystal "B" will create a 90° domain and no 180° domains (Fig. 14a); however, when the polarity of the field is reversed, a good chance exists of finding antiparallel domains inside the 90° domain. (Fig. 14b). The effect of reapplying a positive field is shown in Fig. 14c, while Figs 14d and 14e show the actual appearance of the crystal in polarized and unpolarized light. Notice that the 180° domain geometry can only occur when free charges are available.

If a small AC field of 20 cps is applied, the 90° wall marked (*) (Fig. 14c) will oscillate, bounded on one side by the nearly stationary 180° domains and limited on the other side by whatever limits the motion of a 90° wall. A detailed discussion



d



e

Fig. 14. Successive steps in the formation of a free 90° wall in the [100] crystal "B". Photograph d) with polarized light and e) with unpolarized light correspond to step c).

has been given because this was the only domain configuration for which AC fields could be applied to a 90° wall which was known to be free of intersecting 180° domains and yet constrained to remain in the crystal. It is not an equilibrium situation, and if the frequency is too low or the field strength too high, the 180° domains will move forward and interfere with the 90° wall motion.

Since the wall velocity is zero at both extremes of its oscillation, the wall appears at high frequencies split in two walls. The distance between the two lines is designated as "wall amplitude" (Fig. 15). The 90° wall amplitude as a function of E at 20 cps is plotted for three such 90° walls in Fig. 16a. The critical field for motion is very small. The wall amplitude at 20 cps proves closely proportional to E^2 . Fig. 16b shows the field strength causing a given amplitude of oscillation in its dependence on frequency, and Fig. 16c gives the amplitude as a function of E for 60 cps, 70 and 300 kcps. The minimum field strength for wall motion increases with frequency, that is, the wall amplitude at constant field decreases with frequency.

At 300 kcps and fields above 3.5 kv/cm, crystal "B" heats up beyond the Curie point as did crystal "A". Since temperature change affects the wall amplitude, high frequency-high field strength measurements must be considered with caution.

The divergence of P at a boundary changes rapidly. Hence the behavior of the oscillations at 300 kcps at the edge of the crystal was compared to that in the middle. No significant difference was found; the wall amplitude proved as large at the edge as elsewhere.

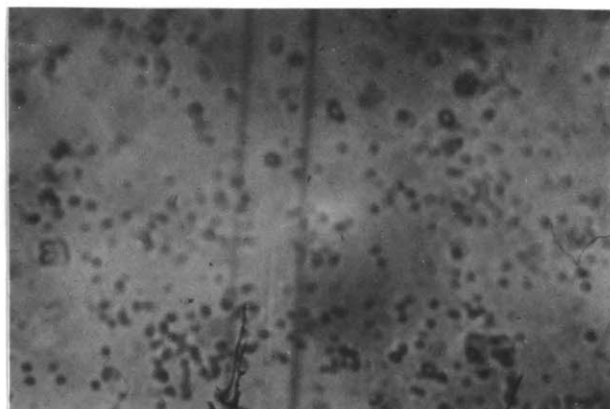


Fig. 15. One 90° wall oscillating in an AC field.
Frequency: 10^3 cps.
Wall amplitude: 8.6 microns.

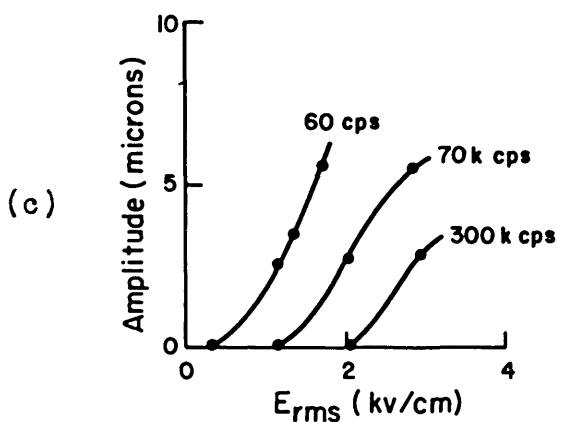
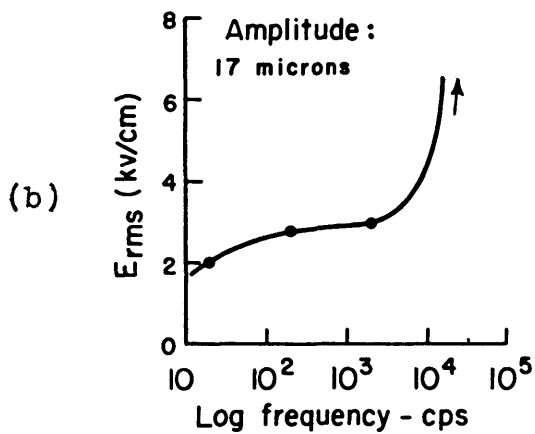
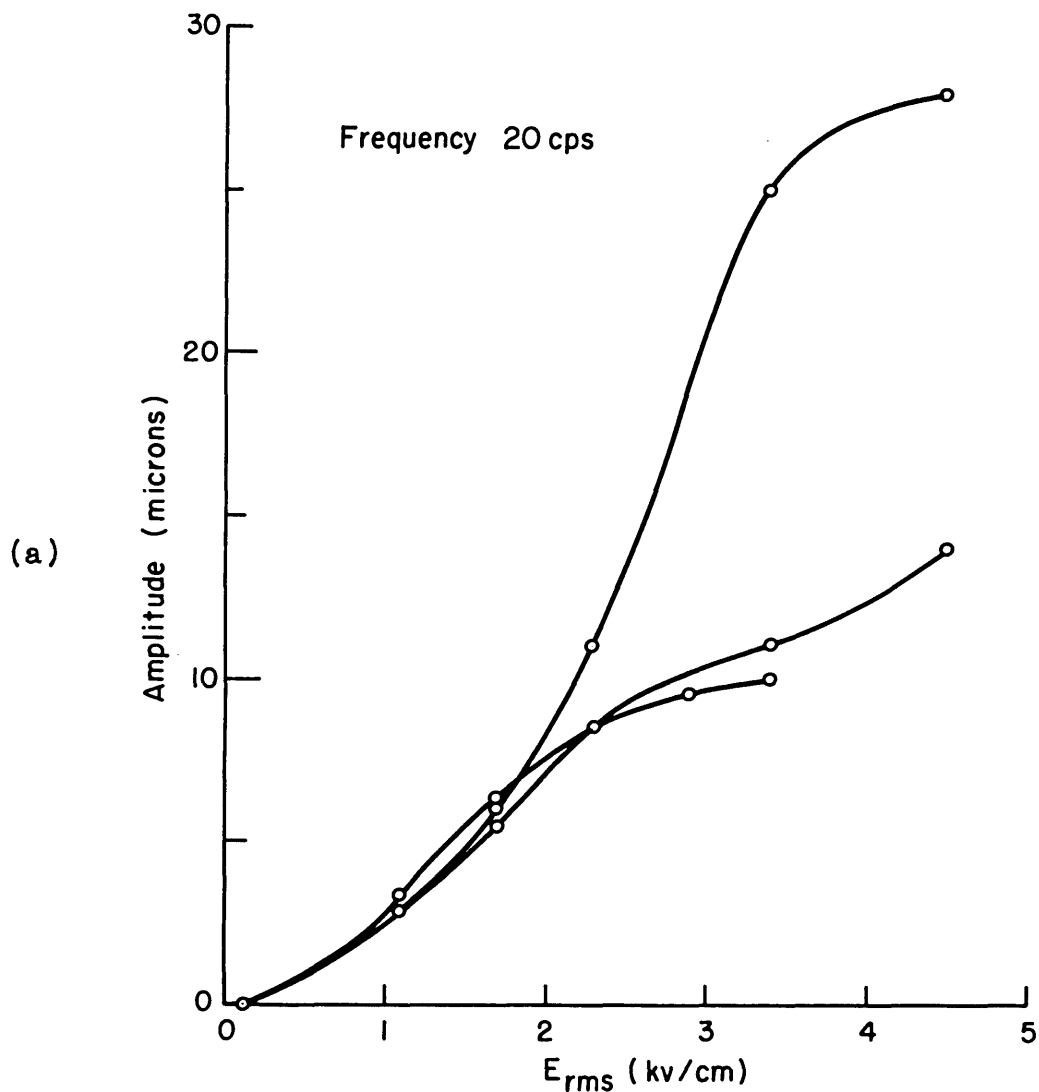


Fig. 16. 90° wall amplitude in AC fields as a function of frequency and field strength.

Discussion

A 90° wall in a field experiences, besides an electrical, a mechanical force. Mechanical stress arises because the $1^\circ 30'$ rotation of the crystal axes across a 90° wall implies that, if the wall moves, the crystal actually changes its external shape. Conversely, if a field through the piezo-effect changes the dimensions of the crystal, 90° domains must be affected. It follows that the geometry of the crystal, the domain pattern, and any external mechanical constraint such as clamping from the electrodes, can affect the motion of 90° walls. The wall velocity is limited by the friction which heats up a rotating crystal as well as by a friction effect evident in the irregular motion of the wall. The wall amplitude is thus very frequency dependent. In contrast to 180° domains, depolarizing fields seem to have little or no effect on 90° wall motion in comparison to the effect of mechanical stress. The trend of the critical field as a function of frequency, neglecting heating effects, suggests that the wall should not be able to move at finite field strengths for frequencies much above three megacycles. The lowest piezoelectric resonance of all our crystals was near 5 to 8 megacycles. Since 90° wall motion depends so strongly on macroscopic mechanical distortions, it is not surprising to find that the wall motion is damped out at a frequency of the order of magnitude of the acoustic resonance frequency.

V. DOMAIN INTERACTIONS

When 90° and 180° domains are simultaneously present and growing in a crystal, the interpretation of observations obviously becomes difficult. However, since we already know some of the properties of each kind of wall, we may hope not only to analyze the interaction, but to obtain additional information about the walls themselves. Although every crystal geometry will have different domain properties, the general behavior can be predicted from a few simple rules most clearly demonstrated in a $[101]$ crystal. In the $[101]$ crystal "C", the same type in which we studied 180° domains - (cf. Fig. 3), but with less strain, 90° and 180° domain nucleation and growth are equally favored.

Beginning our experiments with crystal "C" in the single domain status, we apply a negative DC field and both 90° wedges and 180° wedges are formed and grow, (Fig. 17). After a short time, the 180° boundaries have disappeared but the 90° walls remain. We raise the field further but produce no additional motion. Since the 90° walls might be anchored on imperfections, we check whether or not they are bent or strained; there are no signs of strain. As we raise the field further to as high as 36 kv/cm, nothing happens except that the 90° walls become blurred and difficult to see.

The answer to our confusion is simple in hindsight. Through a complicated process involving 180° domains, which we shall follow in detail, the 90° walls have become head-to-head or tail-to-tail walls. That is, instead of the original head-to-tail configuration

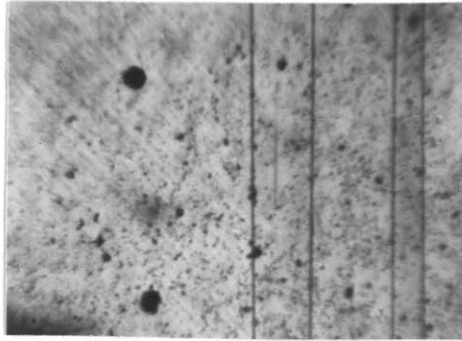


Fig. 17. 90° (and 180°) domains in a $[101]$ crystal.

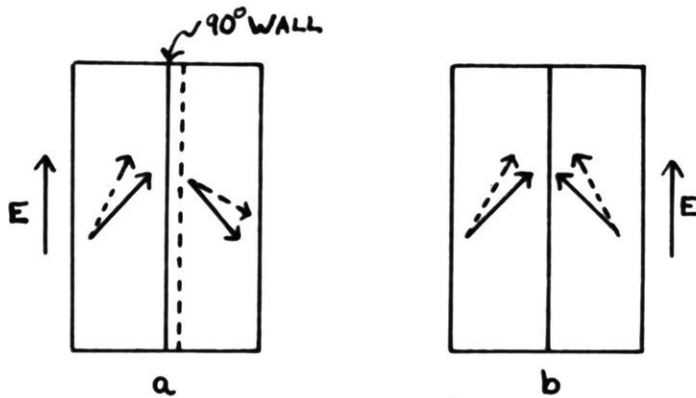


Fig. 18. Effect of field parallel to 90° wall on
a) head-to-tail wall and b) head-to-head wall.

shown in Fig. 18a, the polar axes have become re-oriented as shown in Fig. 18b. As a result no force acts on the walls but only a torque on the dipoles forcing them towards the field direction. This can be verified by measuring the rotation of the extinction axes of adjacent domains; these axes rotated in opposite directions (Fig. 18b). As the field gets larger, the region near the wall rotates so far that the distortion extends over a width of about 5 microns. It appears blurred in nonpolarized light but bright yellow when the rest of the crystal is near extinction.

Again free charges at the 90° wall have neutralized the interfacial polarization that would otherwise produce a large internal field. There is no observable difference in appearance between a head-to-head, tail-to-tail, or head-to-tail wall for magnifications up to 1100X.

A domain configuration as discussed above may be called pseudo-saturated, because, even though there exist 90° domains, they cannot be removed by a realizable field as long as there is a strong electrical anisotropy. Since the polarization of the pseudo-saturated crystal electrically appears the same as it would be if the crystal were a single domain, the two cases cannot be distinguished electrically.

If the field direction is reversed, 180° domains nucleate at the 90° domain boundaries and help to turn the polarization in the opposite direction. The 90° walls, which move only in the stage of head-to-tail walls, can therefore be moved with the cooperation of 180° domains.

Wall Motion in DC Fields

In order to understand the interactions which are occurring, a negative DC field with a rise time of less than 1/100 sec. was applied to crystal "C". A large positive field was applied previously for several minutes to insure that the crystal was initially pseudo-saturated. The motion of a typical 90° wall, as recorded on movie film with the crystal at 45° from extinction, is plotted for two different time scales in Fig. 19(1).

The significant characteristics of typical 90° wall motion are that initially the velocity is very high; next the wall is arrested for about 1/32 sec.; and then it moves on slowly. The slow process nearly fits an exponential relation with a time constant of about $\frac{1}{2}$ sec; a better fit is provided by a relation

$$x = x_0 \ln t/t_0 \quad (7)$$

Finally there may be additional motion for times as long as 30 seconds or even several minutes.

Visual observations made at extinction show the behavior of the antiparallel domains in relation to the 90° wall displacement (Fig. 20a). Since the crystal is initially pseudo-saturated, all the 90° walls are head-to-head or tail-to-tail and no force acts on them when a field is first applied. If the field is just greater than the critical field for nucleation of 180° domains (2 kv/cm), they will nucleate in spikes from the 90° walls and proceed slowly to invert 90° domains. No 90° walls move. If, however, the field is greater than 2.4 kv/cm, and 180° domains have nucleated,

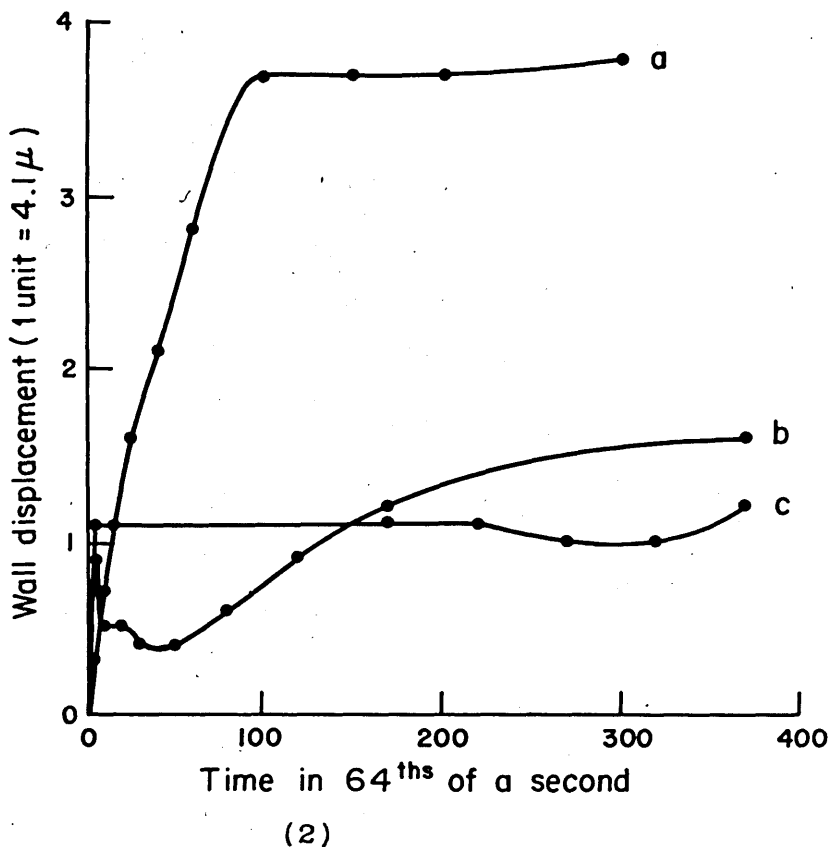
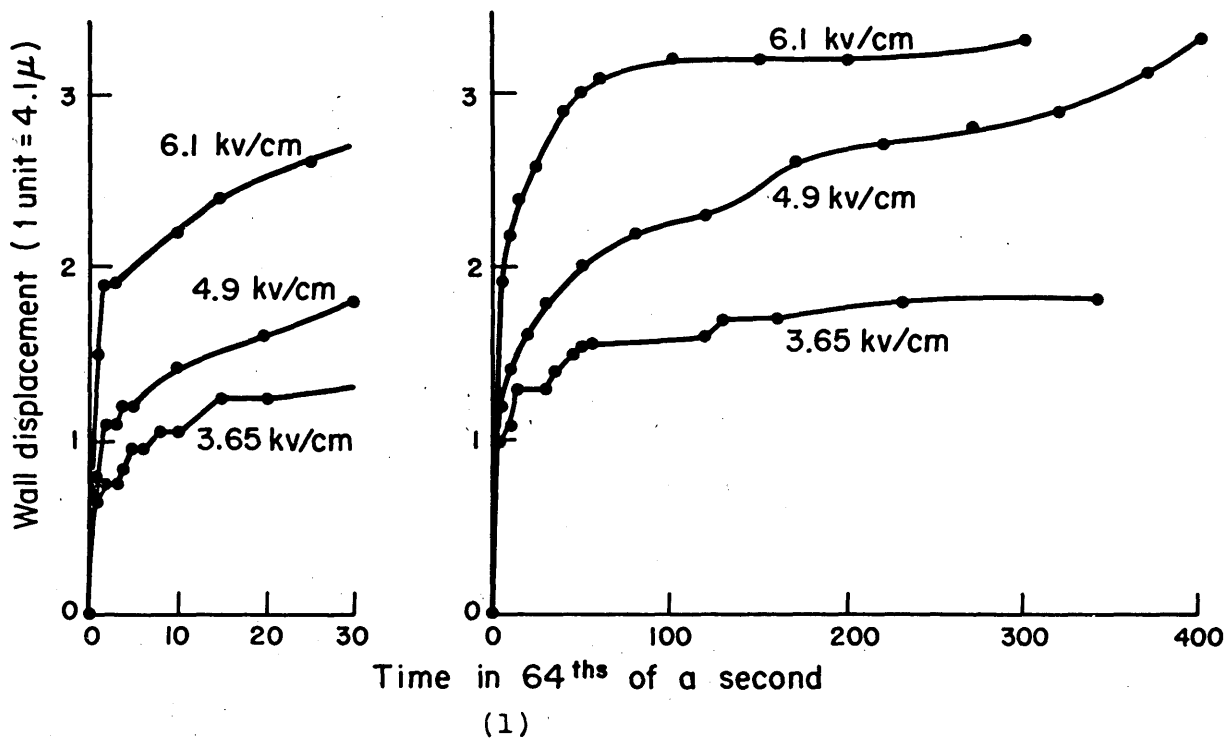


Fig. 19. 90° wall displacement in a DC field as a function of time. (1) represents the motion of a typical wall with two time scales. (2) shows three anomalous walls.

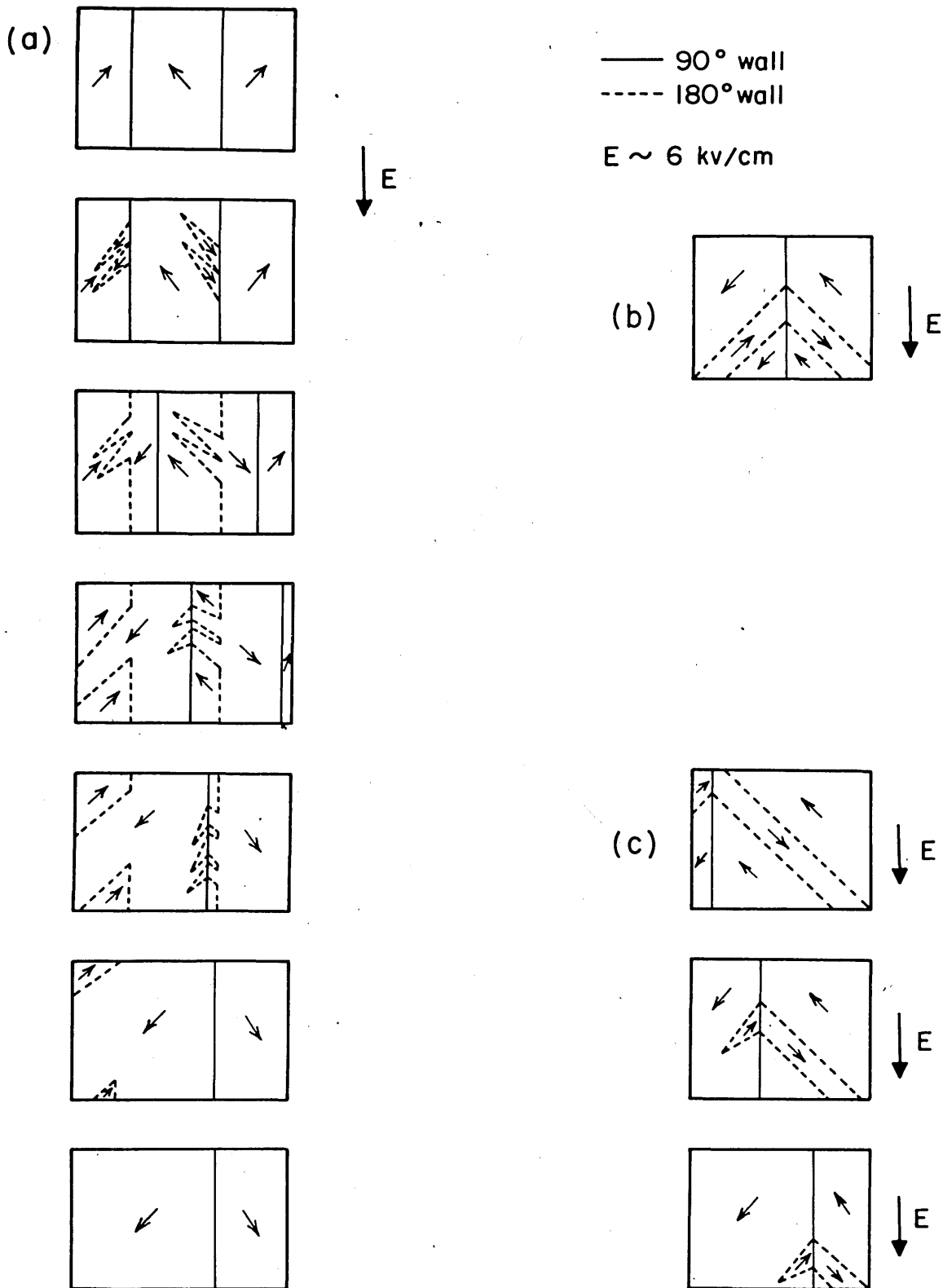


Fig. 20. 180° and 90° domain interactions in a DC field for a [101] crystal. a) sequence of motion for a typical 90° wall. b) an anchored 90° wall. c) a 90° wall telescoping a 180° domain.

there is now a force on the 90° wall and it may break away from its initial position, moving freely and rapidly as a head-to-tail wall until it runs into an obstacle.

Since the position of the obstacle is a function of E , the obstacle is probably 180° domains which are moving forward from the next 90° wall. If a 90° wall with an intersecting anti-parallel domain is forced to move, it must shift the 180° domains sideways through the crystal. This is obviously a difficult process, and the 90° wall is either unable to move (Fig. 20b) or telescopes the 180° domain by dragging its tip along (Fig. 20c). Both cases are observed. In the first case, the 90° wall was slightly bent, but still could not move. In the latter instance, a good deal of strain was observed at the 180° wedge tip as it followed the 90° wall. Considerations of the electrostatic fields at the 180° wedge tip would lead us to expect just this behavior. It therefore seems probable that the 90° wall is stopped soon after it intersects the 180° domains.

The subsequent slow motion ($t \sim \frac{1}{2}$ sec) is caused by 90° walls pushing 180° wedges. As the 180° domains grow, the area of the 90° wall on which an electric force acts decreases and the 90° wall velocity approaches zero. Where the 90° wall comes to a stop depends on the growth rate of the 180° domains and on the field strength. The case of large fields is shown in Fig. 20a. Irregularities in the motion are probably due both to sudden movements or nucleations of the 180° domains and to slight imperfections in the crystal. These little jerky steps are prominently displayed in slow motion pictures and give rise to a ferroelectric Barkhausen effect.

The last part of the motion relates to the final slow disappearance of 180° domains; strain may play a part in determining the final equilibrium configuration in the field, but the end result is complete pseudo-saturation.

A particularly interesting case is displayed at the original position of the 90° wall. The electric charges left behind by the 90° wall are just what is needed to compensate for the interfacial polarization now arising at a 180° wall oriented at 45° to the polar axis. In other words, the head-to-head 90° wall, in order to move, had to change into a head-to-tail wall by creating a 180° wall.

Besides the case just discussed, new 90° wedges will be nucleated for fields greater than 2.4 kv/cm. A thin wedge will enter from one edge and extend across the crystal. Then the two walls will separate and, after a fast, initial displacement, collide with 180° domains.

Since 180° domains can nucleate from any 90° wall on one or both sides of it, there will be a variety of cases (cf. Fig.19-2). Curve (a) corresponds to 180° wedges nucleated on both sides of a 90° wall. The wall therefore is never free to develop a high velocity. Case (b) probably represents a 90° wall winning out against the counteraction of 180° domains. In case (c), a 90° wall moved freely until it reached the charge residue left behind by another 90° wall. Few or no 180° domains were nucleated in the region through which it moved. The slight rearrangement after about five seconds could be due to strain relief.

The total 90° wall displacement during several time intervals summed over all walls as a function of E is shown in Fig. 21. The number of walls is also shown vs. E . At the larger fields, perhaps the existing walls move so fast that new wedges are absorbed before observed. All displacements are increased by increasing E . For fields greater than 4.9 kv/cm, the region of the crystal observed is completely traversed by 90° walls (cf. Fig. 20a). This explains why the displacement approaches a limiting value at the high field strengths.

In summary, we have seen how 90° and 180° domains share in the switching process. The 90° walls move in this [101] crystal because the antiparallel domains play the role of a catalyst.

Wall Motion for Square Pulses

In a slightly different experiment, the fast process was studied. A negative square pulse (height 6.8 kv/cm) was applied to the initially pseudo-saturated "C" crystal. Fig. 22 shows the resultant displacement summed over all 90° walls as a function of pulse length. The number of moving walls decreases with pulse length from about 6 at 1 sec. to about two for times below 1/100 sec. In other words, at short times only 90° walls not hampered by 180° domains move. Additional proof for this analysis comes from the observation that, if the crystal is not originally pseudo-saturated, that is, if 180° domains as well as 90° domains exist in the crystal, pulses shorter than 1/100 sec. barely move any 90° walls.

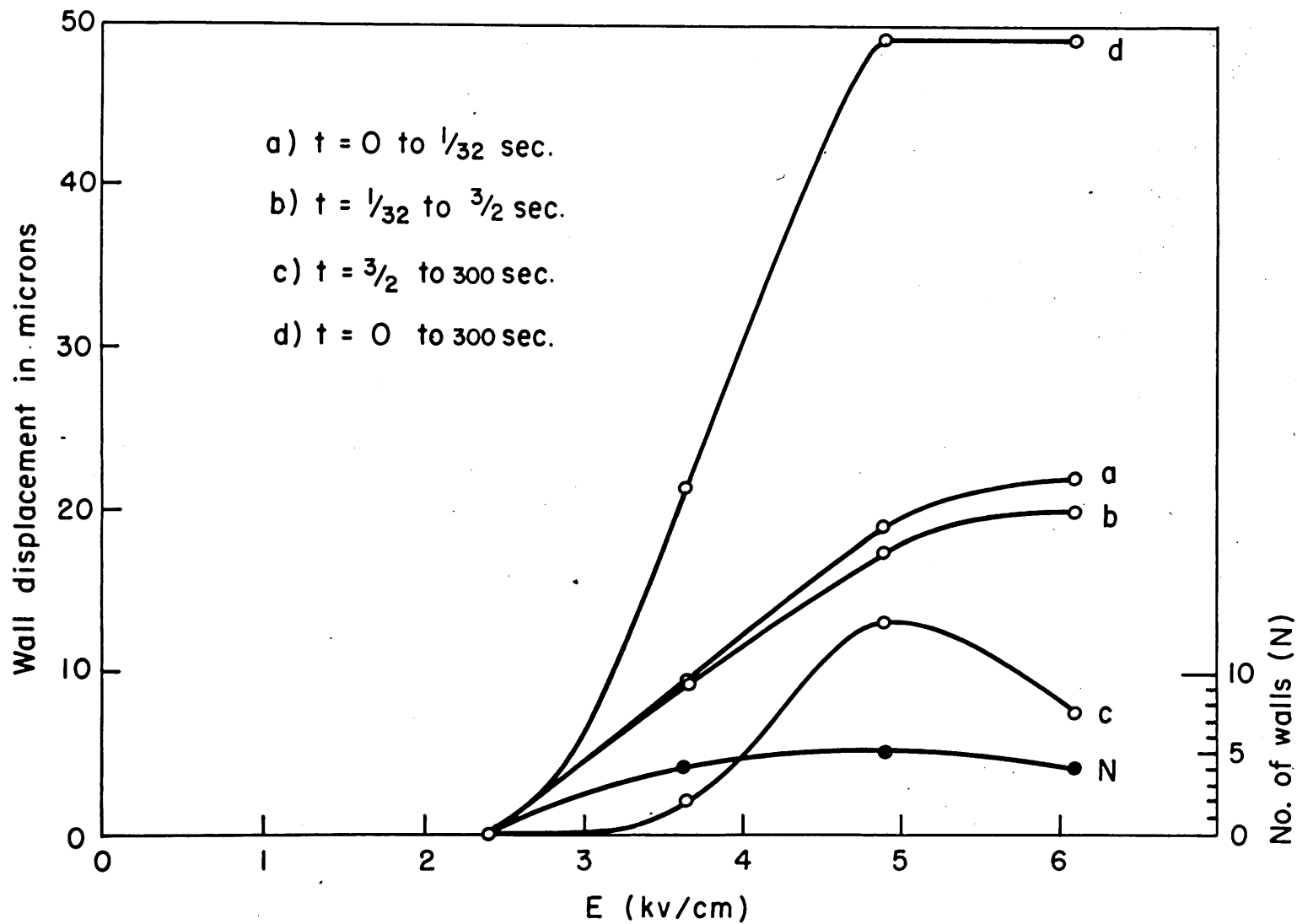


Fig. 21. Total 90° wall displacement in a DC field during specific time intervals as a function of field strength. The number of walls which move is also shown.

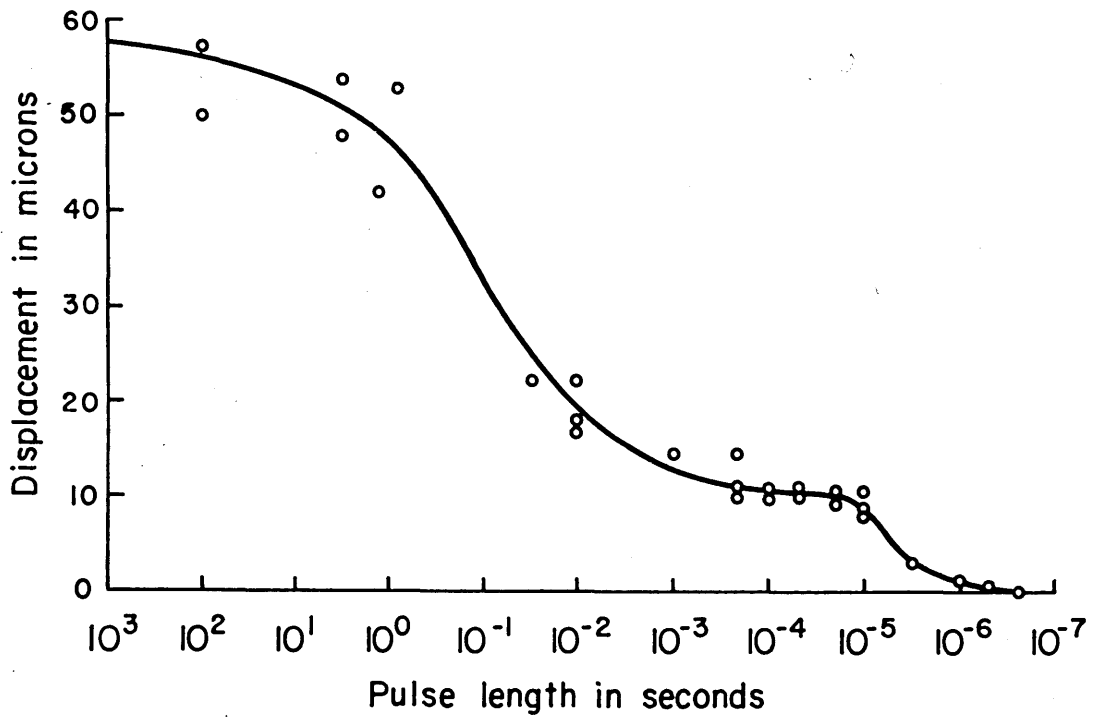


Fig. 22. Total 90° wall displacement caused by a square pulse of height 6.8 kv/cm as a function of pulse length.

For pulses less than one microsecond, only wedge tips move. We deduce as we already established previously that the velocity of a wedge tip is greater than the sideways velocity of a 90° wall.

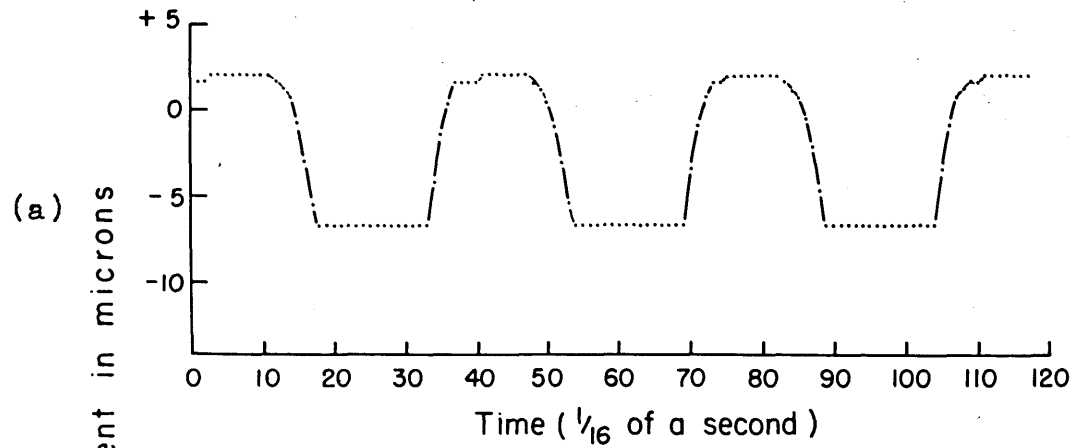
As the pulse length shortens below 10 microseconds, the displacement of any wall drops rapidly to zero. A value of about 10 microns/10 microseconds (100 cm/sec.) for the sideways velocity of a free 90° wall at 6.8 kv/cm appears to describe the situation.

We conclude that 90° walls move at 100 cm/sec. until they hit the 180° domains; then they continue with a much decreased velocity until the crystal is pseudo-saturated.

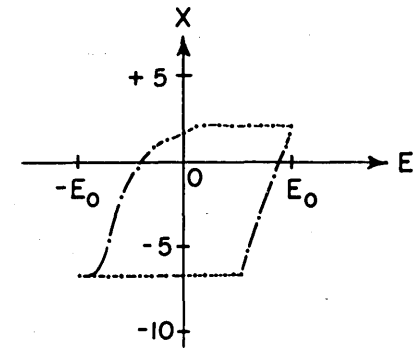
Wall Motion in AC Fields

There is some statistical element in 90° wall motion, probably connected with the 180° domain nucleation process. Observations in high frequency fields make it easier to average out these fluctuations. For this reason AC fields of various frequencies were applied to the [101] crystals.

Fig. 23a shows the displacement of a 90° wall in a low frequency AC field as a function of time and field strength. (The measurements were taken from movie film). Obviously, this wall behaves like the wall of Fig. 20a. After the crystal is pseudo-saturated in the negative direction, a critical positive field of 1.5 kv/cm is required to form 180° domains and separate the 90° wall from its compensating charge. It then moves rapidly until it meets 180° domains. When the field is reversed, the wall returns to its original position. No critical field is observed on the return trip; this implies that, although 90° wall motion appears

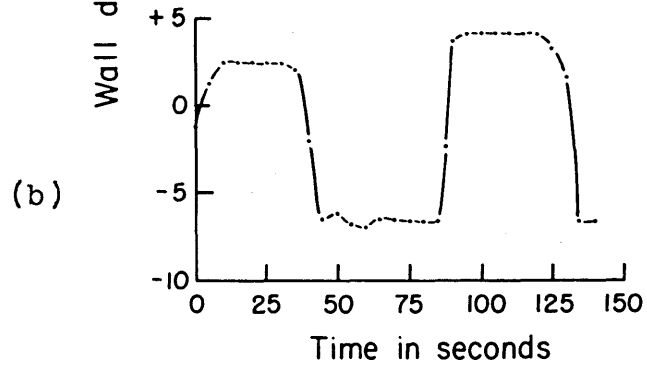


$$\nu = 0.046 \text{ cps}$$



$$E = E_0 \sin 2\pi\nu t$$

$$E_0 = 2.7 \text{ kv/cm}$$



$$\nu = 0.0115 \text{ cps}$$

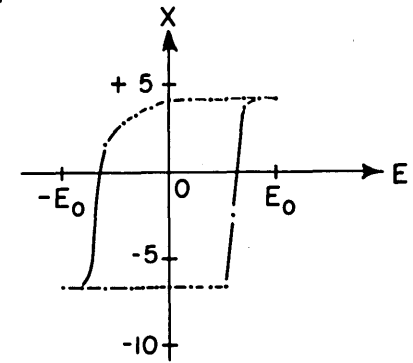


Fig. 23. 90° wall displacement in an AC field as a function of time and field strength. (a) 0.046 cps and (b) 0.0115 cps.

to stop, the crystal does not pseudo-saturate in the positive direction even at this low frequency. The wall displacement vs. E represents a hysteresis loop.

Fig. 23b, for a lower frequency, shows two significant additional facts: the initial velocity of the wall is lower at the lower frequency, probably because of the decrease of $\frac{dE}{dt}$ with frequency, and the amplitude increases as the frequency decreases. Furthermore, the amplitude requires many cycles to reach a constant value.

Fig. 24a shows the frequency dependence of the 90° wall amplitude for frequencies from 10^{-2} to about 10^6 cps. The data were taken in the sequence a→b→c→d→e. The amplitudes on section a→b increased very slowly with time.

This dependence on time and prehistory makes AC measurements difficult. Fig. 24b gives the amplitude as a function of frequency for several field strengths and Fig. 24c the amplitude as a function of E for several frequencies. It is obvious that the two sets of data are not identical; the arrows indicate the order of measurement.

The low intensity of stroboscopic illumination near extinction makes it difficult to watch 180° domains move in AC fields. However, we know that at high amplitudes the 90° walls run into 180° domains and are slowed down or stopped. We also know that 180° domain nucleation increases with $\frac{dE}{dt}$. Therefore as the frequency decreases, the 90° domains must be able to move further before meeting 180° domains. The time dependence arises because

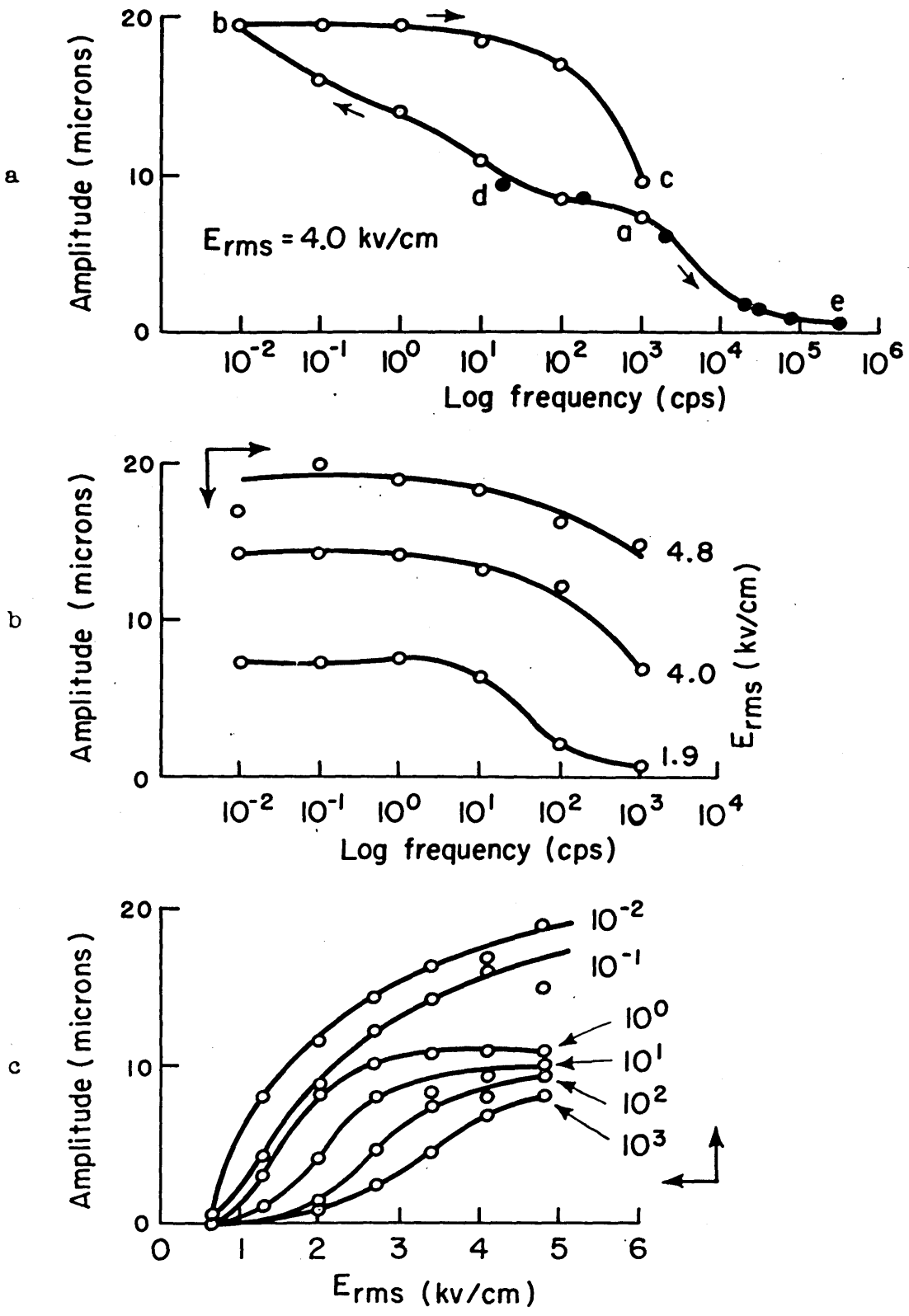


Fig. 24. 90° wall amplitude in AC fields as a function of frequency and field strength.

the crystal was not pseudo-saturated with a DC field before each new frequency was applied and the interacting 90° and 180° domains require time to reach an equilibrium.

One can sometimes observe a 90° wall anchored at some place but oscillating somewhat over the rest of its length. This illustrates the rigidity of 90° walls.

Although no effect of strains causing restoring forces were found in the $[101]$ crystal discussed thus far, other $[101]$ samples showed marked strain effects. In such a crystal, AC fields cause 90° walls to drift together and to disappear. Strain effects seemed to occur preferentially in thicker crystals.

An important result of these experiments is the realization that 90° wall motion in a $[101]$ crystal is intimately connected with antiparallel domain motion.

Temperature Effects

Figure 25 shows the 90° wall amplitude at 60 cps as a function of temperature in a $[101]$ crystal for several field strengths. The amplitude goes through a slight minimum near 60°C . as the temperature increases from room temperature to about 100°C . At temperatures above 80°C , the number of 90° domains suddenly increases tremendously (Fig. 26). Double ended wedges nucleate in the body of the crystal and the domain walls often become too dense for counting. These effects are most prominent at high field strengths. This abundance of 90° domains, which makes it difficult to study other temperature effects in our crystals, appears to be caused by the lowering of the energy barrier for rotation (Appendix A)

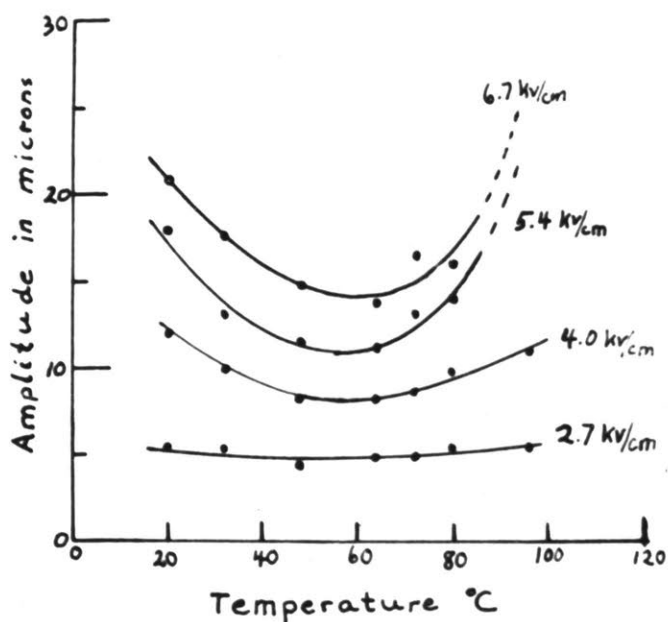


Fig. 25. Dependence of 90° wall amplitude on temperature in a 60 cycle AC field.

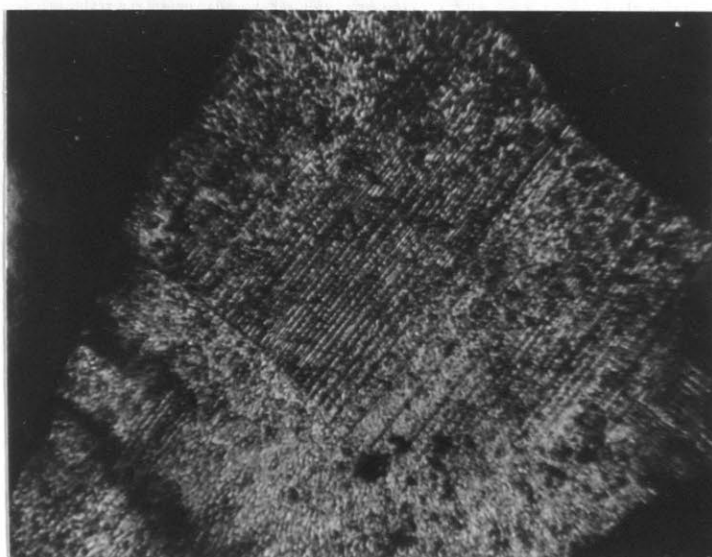


Fig. 26. 90° domains which appear in a [101] crystal if a field is applied at temperatures above 80°C. (Same crystal as that of Fig. 3.)

and a decrease in the 90° wall energy at high temperatures. Less than 10°C from the Curie point, the wall energy is apparently so small that a 90° wall can bend as much as 4° from its original $\{101\}$ plane. The wall at high temperatures appears nearly isotropic - i.e., black in polarized light but transparent and hard to see in unpolarized light.

One reason for the existence of a minimum near 60°C could be that the behavior of 180° domains changes with temperature. However, the shape of the curve of the 90° wall amplitude as a function of temperature is similar to the curve of the dielectric constant, ϵ_a vs. T , (10, see also 14). Since the ease of rotation of the dipoles is reflected in the piezoelectric shear of the crystal (Appendix A) as well as in the dielectric constant, we may have here evidence of the effect of lattice distortions on the motion of the 90° walls.

VI. ADDITIONAL OBSERVATIONS

Rotation of Optical Axis

Measurements of the rotation of the optical axis, θ_0 , as a function of the electric field for several crystals are given (Fig. 27). θ_0 is a linear function of E for angles as large as 10° . We show in Appendix A that for small θ_0 ,

$$\theta_0 \sim \frac{\epsilon_a E_x}{P_s} . \quad (8)$$

Crystal "B", which showed the fewest strain effects in domain experiments, has the largest slope $\frac{d\theta_0}{dE}$. From the slope of θ vs. E for "B", letting P_s be 0.25 coul./m^2 and χ_a be 5000, we find

$$\theta_0 = 1.4 \frac{\epsilon_a E_x}{P_s} . \quad (9)$$

In crystal "A" there was previously observed a built-in strain, due perhaps to clamping by the electrodes or to an imperfection. The rotation of the optical axis in an electric field is lower than that for crystal "B".

While the field in crystals "A" and "B" had to be less than the critical field for 90° domain nucleation, crystal "C" was a [101] crystal and when pseudo-saturated, the field could be as large as practical short of breakdown without nucleating domains. There were some 90° walls initially present in "C". At higher field strengths the center of a domain was rotated more than the

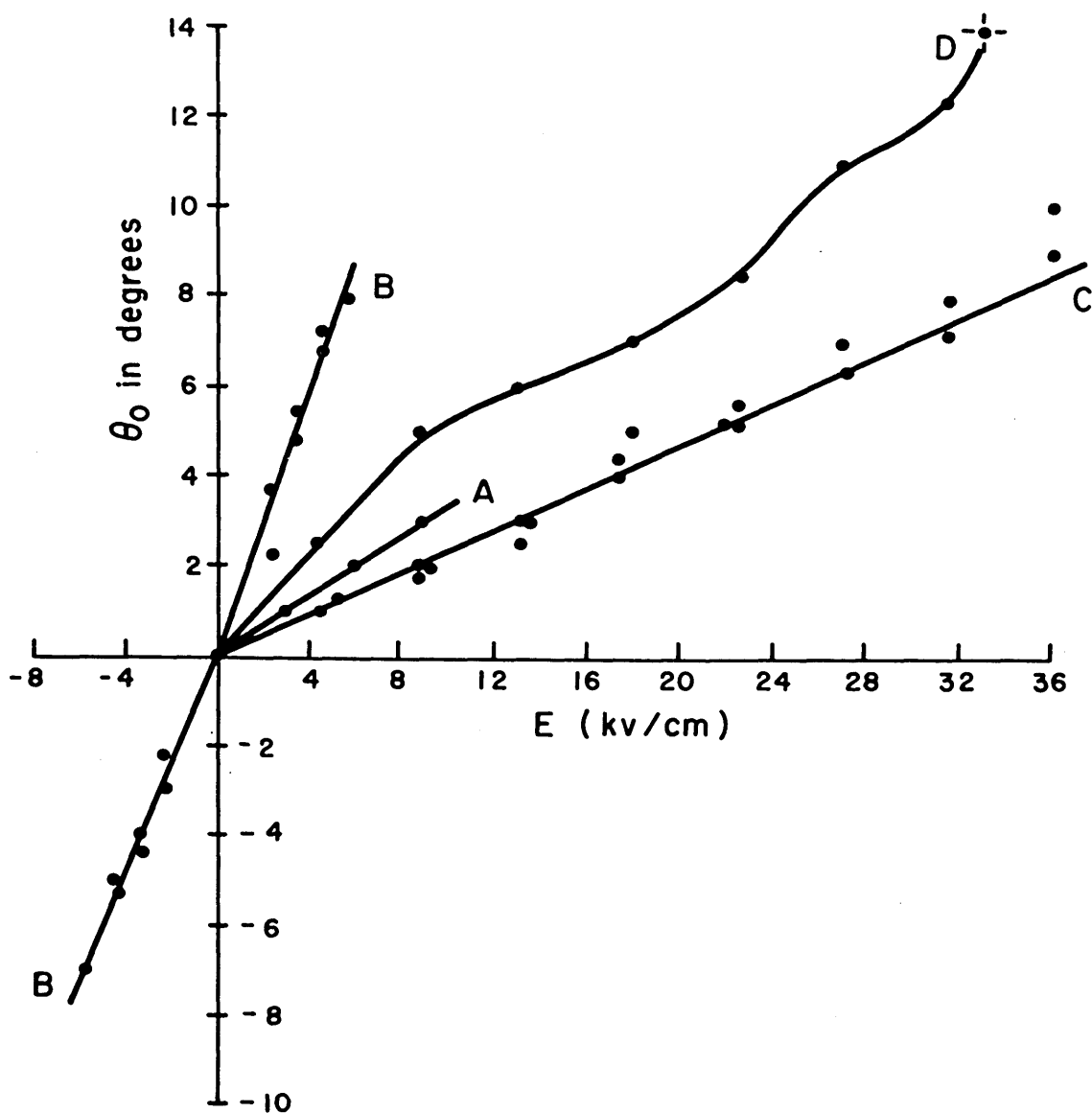


Fig. 27. Rotation of extinction direction, θ_0 , as a function of field strength.
 A: [100] crystal "A".
 B: [100] crystal "B".
 C: [101] crystal "C" at 25°C.
 D: [101] crystal "C" at 15°C.

region near the walls. Measurements were taken at the center of a domain. From the low slope of θ_0 vs. E for curve C, we see that 90° walls inhibit rotation.

The rotation of the optic axis depends on ϵ_a . For crystal "C", lowering the temperature and thus increasing ϵ_a (10) does indeed increase the slope of θ_0 vs. E. Curve D was measured for crystal "C" at 15°C , in contrast to A, B, and C which were measured at 25°C .

At 32 kv/cm in Curve D, domains typical of the orthorhombic phase were nucleated. The walls were indistinguishable from 90° walls but occurred on (001) planes. This reflects the development of a minimum in the free energy for the orthorhombic phase with decreasing temperature. Probably because of the high fields and the stresses set up by foreign domains in the crystal, breakdown occurred and a permanent brown opaque region appeared. When a DC field was subsequently applied, no effects were observed in the rest of the crystal but the brown region heated above the Curie point. It is deduced that the brown region became conducting.

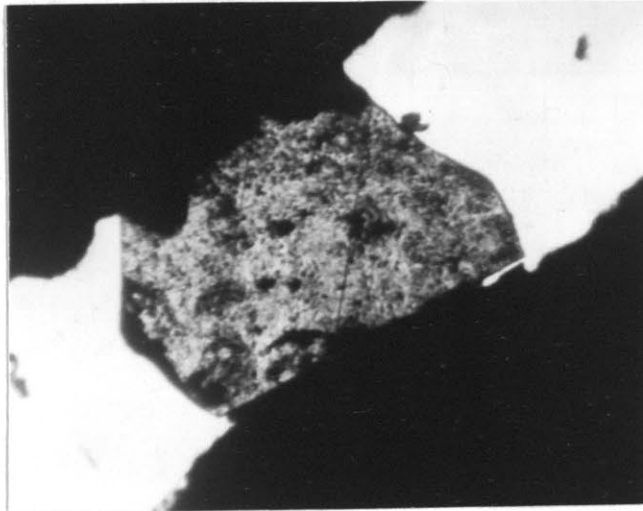
Cubic-Tetragonal Domains

Visual observation of the phase transition at 120°C for tiny "a" crystals indicates the following behavior. Heating from the tetragonal to the cubic phase, the birefringence (color in white light) changes rapidly but nearly continuously. The phase transition starts at several places and no sharp demarcation is seen between the two co-existing phases.

When a crystal is cooled from the cubic to tetragonal phase, the transition occurs more rapidly - i.e., several of the birefringence colors observed for the heating process are not seen. The transition usually initiates in one or more regularly shaped "domains". In several cases, the boundary between a domain of the tetragonal phase and the cubic matrix appeared as a sharp black line indistinguishable from a 90° wall. The phase boundaries occur on a $\{101\}$ twin plane and can be moved forward and back by lowering or raising the temperature. Fig. 28a shows two such lines in unpolarized light in crystal "A". The domain in the middle, as seen in polarized light (Fig. 28b) is cubic, while the outer domains are tetragonal. If the center domain were a "c" domain, the boundaries would have the thickness of the crystal. The existence of an opaque wall shows that the two phases do not have the same lattice dimensions.

Fatigue

While any experiment proved repeatable within the limits of small scale fluctuations at a given time, several days later, repetition of the experiment, while giving qualitatively the same picture, may lead to different quantitative results. Initially one might be inclined to blame electrode contact, but the crystal can often be restored by heating above the Curie point. Since, whatever causes this effect, the maximum activity for a given field strength should present the best data, all experiments were done several times and the lowest field strength values are here reported. Other experimenters (23) have also seen fatigue effects such as a decrease in domain activity with repeated pulsing of the crystal.



(a)



(b)

Fig. 28. Cubic-tetragonal phase boundaries in Crystal "A".
(a) unpolarized light and (b) polarized light.

VII. DISCUSSION

The spontaneous polarization of a single domain crystal of tetragonal barium titanate is directed positively or negatively along one of the original cube axes. No matter which of the six directions P_s assumes, the free energy of the crystal, neglecting surface effects, is the same. However, if an electric field is applied, the free energy changes by $-\vec{P}_s \cdot \vec{E}$. If the polarization is originally opposite to the field, the free energy of the crystal can be reduced by reversal of the polarization. This provides the driving force for the switching process. Since there is an activation energy between these states, reversal will not occur unless the barrier can be surmounted or circumvented. We show in Appendix A that surmounting of the barrier requires a field of about 12 kv/cm for rotation and 80 kv/cm for reversal of the titanium position. Since much lower fields suffice in practice, some other process, domain formation, must be responsible. That there still remains a barrier is evidenced by the existence of a critical field E_c of about 2 kv/cm for good single domain crystals. We suggest that this barrier represents the energy required to form a domain.

This last statement is fundamental to an understanding of the switching process. That there exist imperfect crystals with coercive fields of 30 kv/cm or more only proves that interlocking domains and crystalline imperfections can "work harden" the crystals. We are here interested in the ideal case in which the critical field is the minimum field strength for domain formation.

We have to distinguish furthermore between the formation of domains and the motion of domain walls.

In any real crystal there are imperfections. If a domain can form more easily at an imperfection than elsewhere, the measured critical field and activation energy will be lower than that predicted by any theory. It will be recalled that anti-parallel domains generally appear in the same place every time. The 90° domains were so close together that although they appeared in the same area each time, it cannot be stated definitely that their origin was uniquely determined. However, it is highly probable that both kinds of domains start at imperfections.

In order to describe the nucleation of domains in more detail, we must describe the domains themselves. In the discussion which follows we draw freely on existing theories of nucleation processes (24) but observe that no existing theory is yet adequate to describe nucleation in solids very satisfactorily. We will consider first the nucleation and growth of 90° domains.

Nucleation and Growth of 90° Domains

Several properties will determine the nucleation of 90° domains. The creation of a 90° domain represents a large (1%) mechanical distortion. The lattice inside the new domain must shear by 90° and the rest of the crystal distort to accommodate it. Therefore, a 90° domain can probably not grow faster than the velocity of sound. This has been already postulated from dispersion characteristics (20) and from the theory of plastic flow (25).

Aside from the mechanical distortion much exaggerated in Fig. 29, there is an electrical dislocation produced at the wedge tip. Therefore the growth of a 90° domain can be visualized as the advance of a wedge tip dislocation. The difference between Fig. 29 a and b lies in the sign of the dislocation. The first case (Fig. 29a) was not observed, except for unusual conditions of temperature or stress.

Although the geometrical picture of domain growth may be the same at all stages, nuclei obviously grow in a different climate until they reach a stable size. Since individual walls are perhaps $\frac{1}{2}$ micron thick, a wedge of only $\frac{1}{2}$ micron width would be all wall. It is important also to remember that dipole interactions have a relatively long range.

Below a critical size the energy of the crystal is raised by the growth of a wedge rather than lowered. The decrease in crystal energy due to the formation of a domain of volume, V , and surface area, A , is $-P_sEV$, but the increase in energy due to the formation of walls is σA , where σ is the wall energy. If the domain is a long thin wedge extending through the thickness of the crystal, d , (10 microns) with a wedge length, l , and a width at the base, w , then $w = 2l \tan \theta$ where the wedge angle θ is a constant and about 10^{-2} radians according to observation. The change in crystal energy, ΔU is

$$\Delta U = -P_sEV + \sigma A = -P_sE d l^2 \tan \theta + \frac{2\sigma d l}{\cos \theta} \quad (10)$$

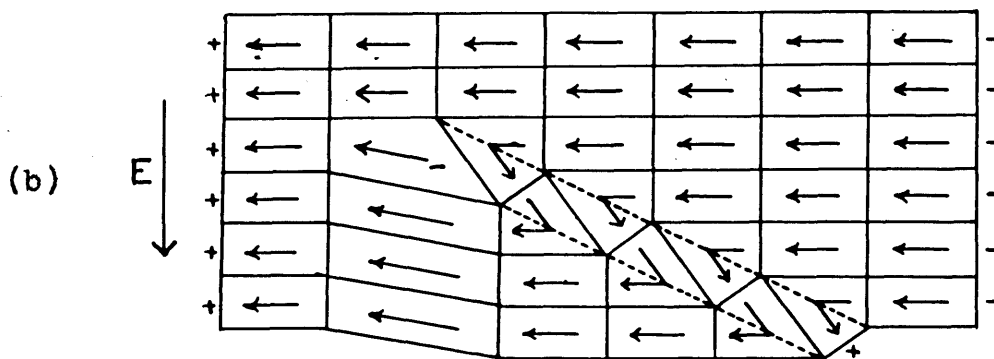
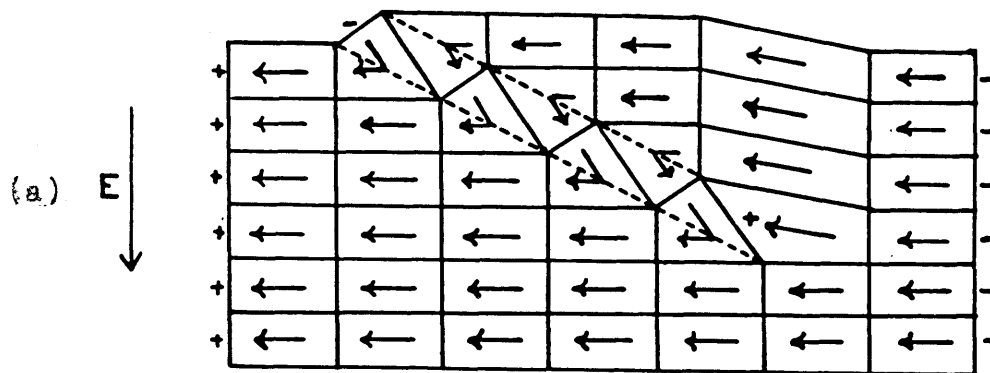


Fig. 29 . Model for 90° wedge showing both mechanical and electrical distortion.

Thus ΔU will increase as l increases if l is less than a critical length l_c . In order to find the critical length, we

set $\frac{d\Delta U}{dl} = 0$ and obtain

$$l_c = \frac{\sigma}{P_s E \sin \theta}$$

For $\sigma \sim 10^{-1}$ joules/m² as calculated in Appendix B, and $E = 7$ kv/cm, $l_c \sim 50$ microns and $w_c \sim 1$ micron. This critical size is of the order of magnitude estimated by visual observation of the wall thickness.

The preceding discussion shows that a wedge becomes stable and grows by the action of the field when it reaches a critical size. Next we ask how the wedge reaches this size.

Since it cannot reach the critical size in one fluctuation, it must grow by individual switching acts. At any time there will be at dislocations some 90° dipoles. In a field their number will increase, and if the field is greater than E_c , a nucleus has a chance of growing beyond the critical size.

Two refinements have to be made. There will be a finite time required for the size distribution of incipient nuclei to reach equilibrium if at $t = 0$ a field is applied. The number of nuclei of a critical size would therefore be zero for a finite period and then increase with time to a constant value. Furthermore, since the domains nucleate at imperfections, the nucleation rate will decrease as these sites are exhausted. Hence an initial increase and then a decrease in the nucleation rate with time is expected and observed. If we divide the length of the wedges when observed, 500 microns, by the minimum incubation time in the limit of high fields, $t_s \sim 0.05$ microseconds, (Eq. 2), the limiting growth velocity, 10^6 cm/sec. appears to be of the order of sound velocity. After the incubation period, the measured

nucleation rate increases rapidly to

$$\frac{dN}{dt}_{\max.} = 5.6 \times 10^6 e^{\gamma E} e^{-\frac{B}{E}} \text{ sec}^{-1} \quad (11)$$

and then decreases with $1/t$.

Since the nucleation rate has its maximum value at the onset of nucleation, statistics which apply only to equilibrium conditions may not hold here.

After a 90° wedge has been introduced and extended across the crystal, the domain dynamics become different. All evidence points to the fact that a 90° wall is quite thick and its motion is not a process of discrete molecular steps. The limiting field for motion is low and strains obviously play an important role. Electrostatic fields arising at the surface of the crystal where the polarization changes by the wall motion, seem to be less important than strain in determining the wall motion. Closely related to this behavior is the fact that the 90° wall is quite rigidly confined along a $\{101\}$ plane, in contrast to the behavior for the 180° domains.

Nucleation and Growth of 180° Domains

The most probable model for a 180° wall is a $\{100\}$ twin plane across which the polar axis changes abruptly by 180° . Not only do theoretical considerations - c.f. (15) - show that the strongest dipole interactions are along the polar axis, but the best thermodynamical theory at present available predicts even antiferroelectricity (26). In addition to the electric interactions,

mechanical coupling (27) tends to maintain the lattice in its tetragonal form through the wall, and the electromechanical coupling operates to maintain the dipoles only parallel or antiparallel. If the dipole moment would rotate through 180° or change in magnitude in a continuous manner through the wall, large mechanical and electrical distortions would result at the wall. However, in contrast to a 90° wall, we observe no distortion at an unstressed 180° wall.

For such a wall to move perpendicularly to the polar axis requires that the dipole moments in a whole column simultaneously switch over or rotate through 180° . Either motion is obviously difficult, since it involves high activation energies. But there is an easy way for the wall to move similar to the propagation of a dislocation, in which one cell at a time reverses polarity and the "flip" propagates along the column of the strongly coupled oxygen-titanium ions. In this manner only one cell at a time is distorted. The velocity of the wall along the polar axis depends on the propagation velocity of a "flip" and the velocity perpendicular to the axis on the rate of nucleation of additional "flips" (Fig. 30). Although a discussion similar to that for 90° wedge nucleation must apply also to 180° domains, there will be significant differences. Because of the different wall geometry, the critical nucleus will have a different shape and size. Also, because - in contrast to 90° domains - nucleation and widening involve the same mechanism of "flips", it is difficult to separate nucleation and growth processes. The fact that about the same limiting field is observed for nucleation and growth is in line with this observation.

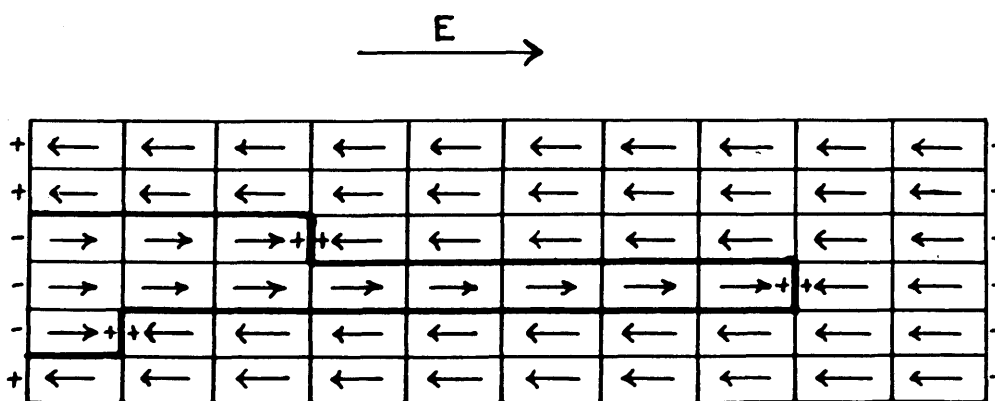


Fig. 30. Model for 180° wedge showing electrical distortions.

Some General Observations

While 90° domains are very interesting, and their study has yielded much useful information, their coupling to 180° domains and the inherent asymmetry of a 90° domain switching process make 90° domain dynamics complex. 180° domains, on the other hand, in a "c" crystal can appear alone and the switching process is a simple inversion effect.

Since the behavior of domains appears to be very sensitive to the conductivity of the crystals, variations of the conductivity might prove an important means for shaping the hysteresis loops and controlling domain dynamics (c.f. - 20). Such effects as humidity and photo-sensitivity should be investigated not only for their practical importance, but to learn more about the origin and properties of the free charges in barium titanate.

It is interesting to note that antiparallel domains in Rochelle salt (21), which are not quite antiparallel due to lattice distortions, have some of the properties of our 180° and 90° domains. Their properties appear to depend both on strain and electrostatic fields.

At the completion of this study, the author received a pre-publication copy of research done by Mertz (28) on antiparallel domains. In essence Mertz measured the maximum current, i_m , and switching time, t_s , for barium titanate "c" crystals in a DC field. Although the crystals he used were "doped" to reduce conduction, and our optical observations concern "a" crystals, a correlation between our results should be possible. Mertz concludes that, rather than

domain wall motion, there are two other processes: propagation of a spike along the polar axis and nucleation of new spikes, which describe 180° domain dynamics. His data show that at low fields, the maximum current, i_m , is proportional to $e^{-\frac{\alpha}{E}}$ for five decades of i_m . His interpretation is that this relation measures the rate of nucleation of new spikes, ($i_m \sim \frac{dn}{dt}$). This might correspond to the behavior of 90° domains described here. For fields higher than 5 kv/cm, Mertz finds $i_m \sim E - E_0$ and concludes that for this range of field strengths, the average velocity of the spikes along the polar axis is measured. At 5 kv/cm, a velocity of 1.2×10^4 cm/sec. is found, which is within the limits of our values. We also found a similar relation for domain growth. The most significant departure from our results is that spikes appear to nucleate more readily than wedges grow. Since, in a crystal of low conductivity, very little free charge is available to neutralize the closing fields and allow the domains to widen, this result is consistent with our findings.

VIII. SUMMARY

Optical experiments on 180° and 90° domains have provided quantitative data and a descriptive framework for the growth of domains in barium titanate.

Antiparallel domains are introduced into a crystal as long thin spikes with a very high initial velocity. By accumulating compensating charges on the ends of the free dipoles at the domain boundary, the spikes can widen slowly to form wedges. All considerations lead to the postulate that the 180° wall is very thin. The most important single factor for 180° domain dynamics appears to be the conductivity of the crystal.

The growth of 90° wedges represents a nucleation process for which the nucleation rate has been directly measured. The rate of nucleation traverses a maximum as a function of time, and the growth velocity of the wedges appears to approach a limiting value near sound velocity. The 90° wall, in contrast to 180° walls, appears to be quite thick.

In [101] crystals, we investigated the properties of interacting domains. By the cooperation of 90° and 180° domains, a crystal can be switched from a state of pseudo-saturation of one polarity to pseudo-saturation in the opposite direction. Both the long relaxation times and irregularities in the motion represent what probably occurs in a multidomain crystal or barium titanate ceramics.

APPENDIX A

ELECTRICAL, MECHANICAL AND OPTICAL RELATIONS

In a single domain of unstressed tetragonal barium titanate there are three collinear principal axes in the z direction: the c axis, the polar axis and the optical axis. Since barium titanate is a piezoelectric crystal, an electric field, E_x , applied perpendicular to the polar axis can rotate all three of these axes in the zx plane.

Rotation of Optical Axis

The equation (29) of the optical index ellipsoid for an unclamped tetragonal piezoelectric crystal subject to a field, E , in the zx plane is

$$a'_{11}(x^2 + y^2) + a'_{33}z^2 + 2a'_{31}xz = 1 \quad (12)$$

where

$$a'_{11} = a'_{22} = \frac{1}{n_a^2} - r_{13}P_z \quad ; \quad a'_{33} = \frac{1}{n_c^2} + r_{33}P_z \quad ; \quad a'_{31} = r_{15}P_x$$

and r_{ij} are the electro-optical constants of the first order. Note that $P_z = P_s / p_z$, $P_x = p_x = \epsilon_a E_x$ and p_z is very much less than P_s for realizable fields.

To find the principal axes, c' , a' , of the rotated ellipse, we rotate the coordinate axes until the cross term vanishes. In other words, let

$$z = c' \cos \theta_0 - a' \sin \theta_0$$

$$x = c' \sin \theta_0 + a' \cos \theta_0$$

in Eq. (12); set the coefficient of the term in a 'c' equal to zero; and solve for θ_0 . If θ_0 is small, we have

$$\theta_0 \approx \frac{r_{15} p_x}{\frac{1}{n_c^2} - \frac{1}{n_a^2} + (r_{13} + r_{33}) p_x} \quad (13)$$

According to Mertz (10),

$$\frac{1}{n_c^2} - \frac{1}{n_a^2} = P_s (r_{13} + r_{33})$$

Therefore,

$$\theta_0 \approx \frac{r_{15}}{r_{13} + r_{33}} \cdot \frac{\epsilon_a E_x}{P_s} \quad (14)$$

From our measurements on crystal "B",

$$\frac{r_{15}}{r_{13} + r_{33}} = 1.4 \quad (15)$$

Rotation of Polar Axis and Elastic Shear

We consider now the rotation of the polar axis and the crystal shear for an electric field applied perpendicular to the z axis. We will need the expansion of the free energy at zero stress for small distortions from the tetragonal phase.

The free energy, $A_T(x,p)$, is the sum of the elastic, dielectric, and piezoelectric energies for a tetragonal crystal where (29)

$$u_{\text{elastic}} = \frac{1}{2} c_{11}^p (x^2 + y^2) + \frac{1}{2} c_{33}^p z^2 + c_{12}^p xy + c_{13}^p (xz + yz) \\ + \frac{1}{2} c_{44}^p (y^2 + x^2) + \frac{1}{2} c_{66}^p x_y^2 \quad ,$$

$$u_{\text{dielectric}} = \frac{1}{2} \chi''_{11} (\rho_x^2 + \rho_y^2) + \frac{1}{2} \chi''_{33} \rho_z^2, \quad (16)$$

$$u_{\text{piezoelectric}} = a_{15} (x_z \rho_x + z_y \rho_y) + [a_{31}(x+y) + a_{33}z] \rho_z.$$

c_{ij}^p are elastic constants at constant polarization, x , y , and z are strains, χ''_{ii} is the clamped dielectric constant, and a_{ij} are piezoelectric constants. p_x, p_y and p_z are the change in polarization from the tetragonal state where $P_z = P_s$ and $P_x = P_y = 0$. Since we consider E in the x or z direction only, let p_y in Eq. (16) be zero.

We now have the free energy in terms of strains and polarization. Since the stress is held constant, we wish to apply the appropriate Legendre transformation $A_T(X, p) = A_T(x, p) - xX$, to obtain the free energy in terms of stress and polarization, at zero stress.

We find the stress in terms of the strain from Eq. (16).

$$\begin{aligned} X &= \frac{\partial A_T}{\partial x} = c_{11}^p x + c_{12}^p y + c_{13}^p z + a_{31} p_z = 0 \\ Y &= \frac{\partial A_T}{\partial y} = c_{12}^p x + c_{11}^p y + c_{13}^p z + a_{31} p_z = 0 \\ Z &= \frac{\partial A_T}{\partial z} = c_{13}^p x + c_{13}^p y + c_{33}^p z + a_{33} p_z = 0 \\ X_y &= \frac{\partial A_T}{\partial x_y} = c_{66}^p x_y = 0 \\ Y_z &= \frac{\partial A_T}{\partial y_z} = c_{44}^p y_z = 0 \\ Z_x &= \frac{\partial A_T}{\partial z_x} = c_{44}^p z_x + a_{15} p_x = 0 \end{aligned} \quad (17)$$

Solving this set of simultaneous equations for strain, we obtain

$$\begin{aligned}
 x = y &= \frac{[c_{33}^p a_{31} - a_{33} c_{31}^p] p_z}{2c_{13}^{p2} - c_{33}^p (c_{12}^p + c_{11}^p)} \equiv f_1 p_z \\
 z &= \frac{[a_{33} (c_{11}^p + c_{12}^p) - 2c_{13}^p a_{31}] p_z}{2c_{13}^{p2} - c_{33}^p (c_{12}^p + c_{11}^p)} \equiv f_2 p_z
 \end{aligned} \tag{18}$$

$$x_y = y_z = 0$$

$$z_x = -\frac{a_{15} p_x}{c_{44}^p}$$

If now the strains, Eq. (18), are substituted back into Eq. (16), we obtain for zero stress,

$$A_T(\vec{p}) = R_1 p_z^2 + R_2 p_x^2 \tag{19}$$

where

$$\begin{aligned}
 R_1 &= \frac{1}{2} \chi_{33}'' + (c_{11}^p + c_{12}^p) f_1^2 + \frac{1}{2} c_{33}^p f_2^2 + 2c_{13}^p f_1 f_2 + 2p_x a_{13} + f_2 a_{33} \\
 R_2 &= \frac{1}{2} \chi_{11}'' - \frac{1}{2} \frac{a_{15}^2}{c_{44}^p}
 \end{aligned} \tag{20}$$

Moreover, since

$$\frac{\partial A_T(\vec{p})}{\partial p_i} = E_i \quad \text{and} \quad \frac{\partial^2 A_T(\vec{p})}{\partial p_i^2} = \frac{1}{\epsilon_i},$$

an electric field, $E = E_x \hat{x} + E_z \hat{z}$ will rotate the polar axis by

$$\Theta_E \approx \frac{\epsilon_a E_x}{P_s} \tag{21}$$

for small E .

A field will cause - Eq. (18) - a mechanical shear

$$\Theta_M = - \frac{a_{15}}{c_{44}} \epsilon_a E_x . \quad (22)$$

From Eq. (20)

$$a_{15}^2 = \left(\chi_{11}'' - \frac{1}{\epsilon_a} \right) c_{44}^p \quad (23)$$

where (14)

$$\chi_{11}'' \approx \frac{1}{180 \epsilon_0} \gg \frac{1}{\epsilon_a} .$$

Therefore

$$\Theta_M \approx \sqrt{\frac{\chi_{11}''}{c_{44}^p}} \epsilon_a E_x . \quad (24)$$

In the next section we will derive a free energy accurate for all angles of rotation. In a manner identical to the one employed here, we find

$$x_z = \frac{g_{44}}{c_{44}} (P_s + p_z) (p_x) . \quad (25)$$

By assuming (16) that $x_z = 14'$ for $p_x = (P_s / p_z) = P_s / \sqrt{2}$ at room temperature just as it does at -7°C (11), we find

$$\frac{g_{44}}{c_{44}} = \frac{2(14')}{P_s^2} = 0.09 . \quad (26)$$

Now for small fields,

$$\Theta_M = \sqrt{\frac{\chi_{11}''}{c_{44}^p}} \epsilon_a E_x = \frac{g_{44}}{c_{44}} p_x P_s \quad (27)$$

and therefore,

$$c_{44}^p = \frac{\chi_{11}'' P_s^2}{4(14')^2} \approx 1 \times 10^{12} \text{ newtons/m}^2 . \quad (28)$$

This value of c_{44}^P is three times higher than that calculated by Devonshire (16) with the assumption that $c_{44}^P = c_{12}^P$ and a value of P_s which has since been shown to be too low. Measurements on ceramics (30) gave a value of c_{44}^P 20 times lower.

With the calculated value of c_{44}^P ,

$$\Theta_M \approx 0.0065 \frac{\epsilon_a E_x}{P_s} . \quad (29)$$

In summary, we have found that Θ_o , Θ_e , and Θ_M depend linearly on the field E_x for small distortions (Equations (15), (21) and (29)). Θ_o and Θ_e are nearly identical. Θ_M appears to be much smaller. However, Θ_M does not play the same role as an axis of symmetry as Θ_o and Θ_e . The intimate relation between the polar, optical and mechanical axes is apparent. It is the optical axis which is observed visually, the polar axis which is measured electrically, and the mechanical axis which is important in acoustical measurements. This discussion holds only for zero stress.

Free Energy for Rotation

We will now develop the free energy as a function of polarization and stress at zero stress expanded about the cubic phase. Devonshire (16) gives the free energy expanded about the cubic phase as

$$\begin{aligned} A(\vec{x}, \vec{P}) = & \frac{1}{2} c_{11}^P (x^2 + y^2 + z^2) + c_{12}^P (y^2 + z^2 + xy) + \frac{1}{2} c_{44}^P (x^2 + y^2 + z^2) \\ & + \frac{1}{2} \gamma_6'' (P_x^2 + P_y^2 + P_z^2) + \frac{1}{4} \gamma_4'' (P_x^4 + P_y^4 + P_z^4) + \frac{1}{6} \gamma_5'' (P_x^6 + P_y^6 + P_z^6) \\ & + \frac{1}{2} \gamma_{12}'' (P_x^2 P_y^2 + P_x^2 P_z^2 + P_y^2 P_z^2) + g_{11} (x P_x^2 + y P_y^2 + z P_z^2) \\ & + g_{12} [x (P_y^2 + P_z^2) + y (P_z^2 + P_x^2) + z (P_x^2 + P_y^2)] \\ & + g_{44} [y z P_y P_z + z x P_z P_x + x y P_x P_y] . \end{aligned} \quad (30)$$

The difference between this expression and A_T is that whereas A_T only holds for small distortions from the tetragonal configuration, the function we now develop is valid for all phases and configurations of BaTiO_3 . In other words, $A(\vec{x}, \vec{P})$ is a postulated function which, with experimentally determined coefficients, should account quantitatively for all experimentally observable phenomena in BaTiO_3 .

Since the method of obtaining the free energy $A(\vec{X}, \vec{P})$ for zero stress from $A(\vec{x}, \vec{P})$ is identical to that used in the last section, we will give only the results. Again we only consider rotations in the xz plane.

$$A(\vec{P}) = D_1(P_x^2 + P_z^2) + D_2(P_x^4 + P_z^4) + D_3(P_x^6 + P_z^6) + D_4 P_x^2 P_z^2. \quad (31)$$

Mertz (31) has determined from measurements in the z direction that

$$D_1 = 3.7 \times 10^{-5} (T - T_0); \quad D_2 = 1.7 \times 10^{-13}; \quad D_3 = 3.8 \times 10^{-23} \quad \text{in cgs-esu.} \quad (32)$$

T_0 is Curie-Weiss temperature.

D_4 may be determined from the equation

$$\frac{\partial^2 A(\vec{P})}{\partial P_x^2} = \frac{1}{\epsilon_a} = 2D_1 + 2D_4 P_z^2 \quad (33)$$

where $P_x = 0$ and $P_z = P_S$. A more sensitive way is to vary D_4 in Eq. (31) until the temperature at which the free energy of the tetragonal phase, $A(P_S, \Theta = 0^\circ)$, (now in polar coordinates) equals the free energy of the orthorhombic phase, $A(P_S, \Theta = 45^\circ)$, is 0°C . Both methods give $D_4 = 6(\pm 1) \times 10^{-13}$ cgs-esu, but the second

method, being internally consistent, is preferred. We will use the value $D_4 = 5.9 \times 10^{-13}$ cgs-esu. The exact shape of the calculated curves which follow is very sensitive to D_1 , D_2 , D_3 , and D_4 .

Let P'_s be defined as the value of P for which $\frac{\partial A(P, \Theta)}{\partial P} = 0$. In Fig. 31 we plot P'_s against Θ for several temperatures. P'_s is independent of Θ for temperatures near 50°C , but for temperatures above 80°C , P'_s decreases rapidly as Θ goes from 0° to 45° .

Fig. 32a shows $A(P, 0^\circ)$. The minimum obviously occurs at $P = P_s$. In Fig. 32b, $A(P'_s, \Theta)$ is plotted against Θ for several temperatures. At high temperatures, the barrier for rotation by 90° decreases. On the other hand, as the temperature is lowered below 25°C , a metastable minimum develops at 45° which, below 0°C , becomes the lowest energy configuration (orthorhombic phase).

Simplified Free Energy for Rotation

It can be shown that there is one temperature, 55°C , at which P'_s is independent of Θ . From Eq. (31) it follows rigorously that if P'_s is independent of Θ , then

$$A = P_s K \sin^2 \Theta \cos^2 \Theta + K_0 \quad (34)$$

where K_0 does not depend on Θ . Since this equation is simple analytically and is correct for a temperature near room temperature, we may use it as a first approximation of behavior at room temperature.

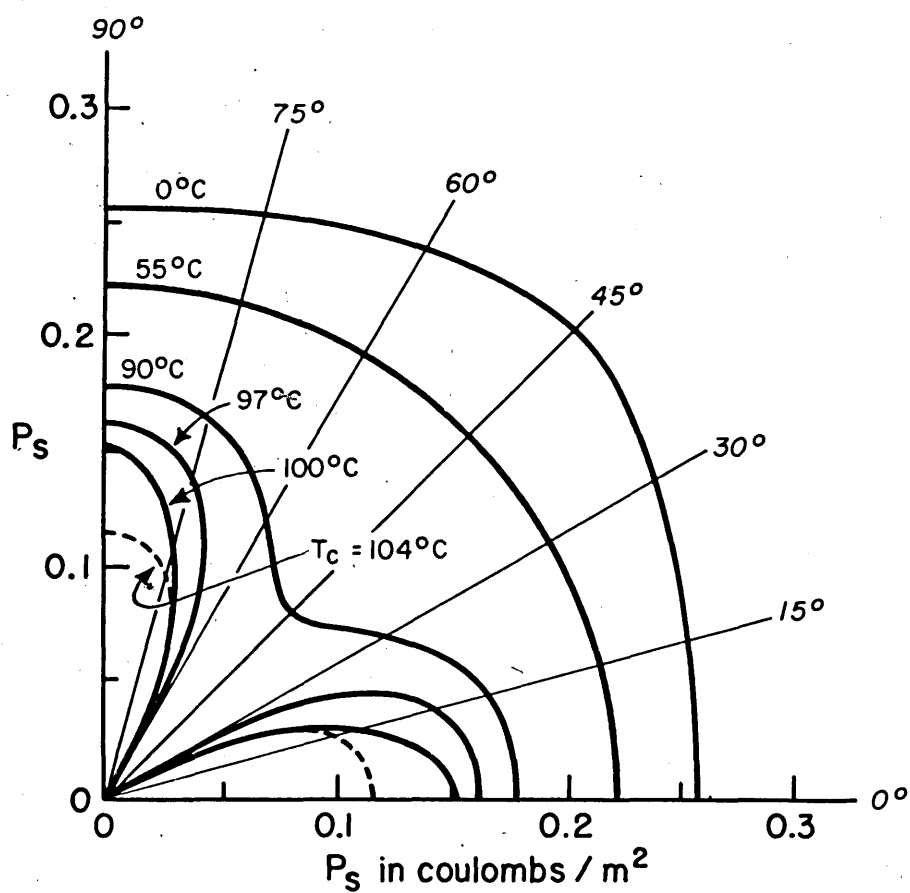
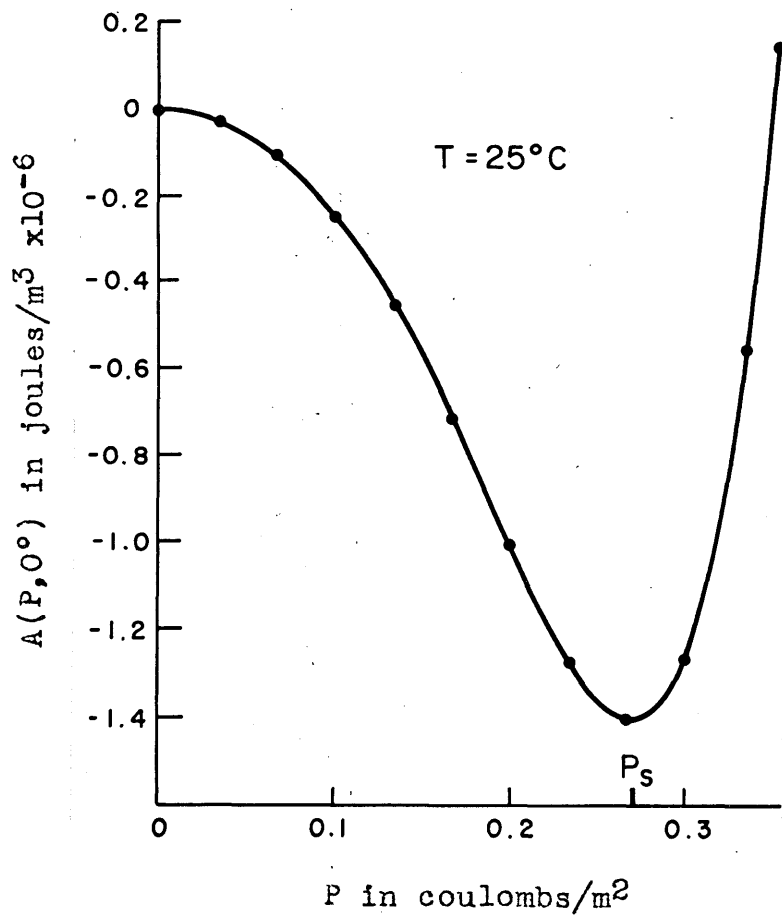
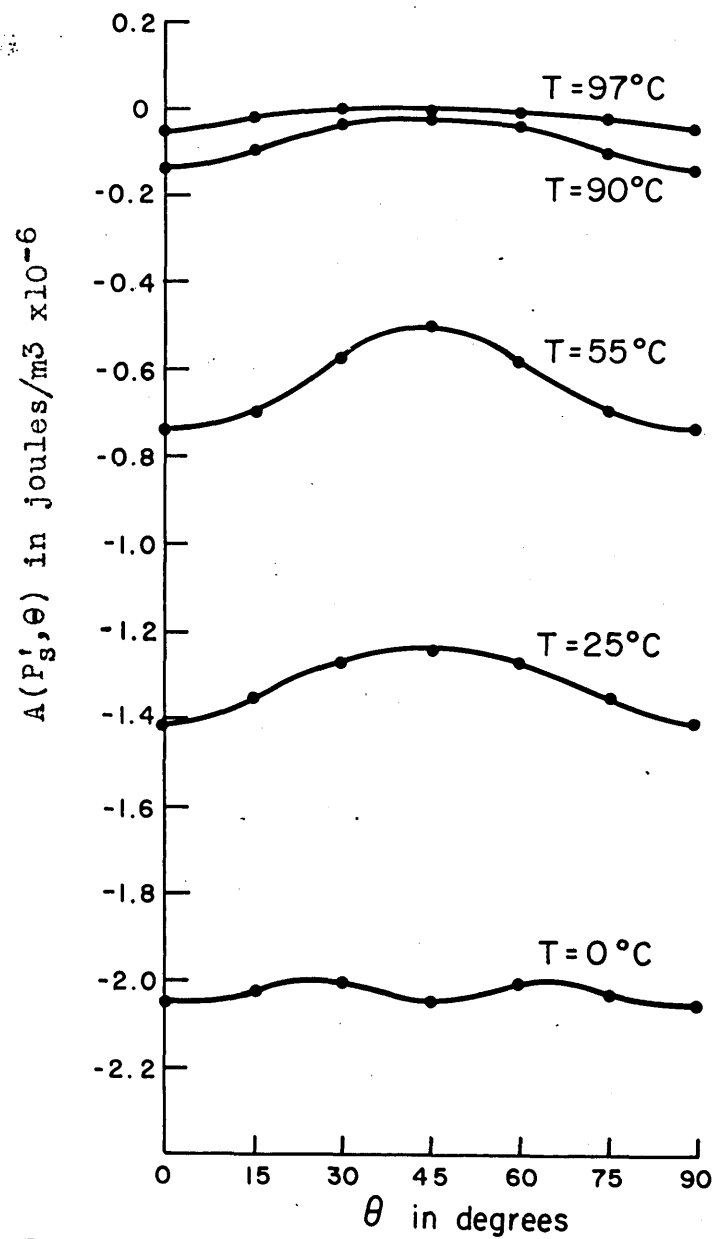


Fig.31. Polar plot of P_s' as a function of θ .



(a)



(b)

Fig. 32. Free energy, $A(P, \theta)$.
 (a) $A(P, 0^\circ)$ as a function of P .
 (b) $A(P_s', \theta)$ as a function of θ .
 θ is measured from the z axis.

Fitting Eq. (34) to the curve of $A(P'_s, \theta)$ at 25°C , we find

$$20 \leq K \leq 30 \quad \text{kv/cm.}$$

The significance of K is that $\sim K/2$ is the maximum slope of the $A(P'_s, \theta)$ curve and therefore 12 ± 2 kv/cm should be approximately the maximum field required to rotate the whole crystal by 90° at 25°C . It is a small field compared to that required to push the dipoles over the barrier in Fig. 32a (about 80 kv/cm).

APPENDIX B
WALL ENERGY

90° Wall Energy

The thermodynamic free energy developed in Appendix A will be a valid representation of the energy per unit volume only for a large region where all the dipoles are aligned. In order to find the energy of a 90° wall, we need to find the energy for dipoles not aligned. We must also consider strong electromechanical coupling and mechanical constraints.

Let us assume that, since the wall is thick, the dipole moment is constant and the dipole angle, θ , varies continuously and linearly through the wall, i.e., $\frac{d\theta}{dx} = \frac{\pi/2}{s}$ from $\theta = 0$ at $x=0$ to $\theta = \frac{\pi}{2}$ at $x = s$, where s is the wall thickness. We will also assume, although because of geometrical constraints this postulate is the most suspect, that the mechanical deformation which is prescribed for each θ at zero stress is realized. For a stationary wall, free charge will neutralize any divergence of P . Therefore, with the above assumptions, the energy density in a small volume in the wall will be $u_1 = P_s K \sin^2 \theta \cos^2 \theta$ (Eq. 34) plus an additional term, u_2 , to account for the variation in θ through the wall. The wall energy per unit area, σ_{90} , will then be the sum of two terms, σ_{u_1} and σ_{u_2} , where

$$\sigma_{u_1} = \frac{2}{\pi} K P_s s \int_0^{\pi/2} \sin^2 \theta \cos^2 \theta d\theta = \frac{K P_s s}{8} \quad (35)$$

σ_{u_1} will be a minimum if the wall is thin. Since σ_{u_2} must represent a force tending to align the dipoles, σ_{u_2} will be lower for a thick

wall. Let us postulate an energy of the form

$$\sigma_{u_i} = \frac{b \pi^2}{4 a s} \quad (36)$$

where b is a constant, and a the lattice spacing $4A^\circ$.

Then

$$\sigma_{90} = \frac{K P_s s}{8} + \frac{b \pi^2}{4 a s} \quad (37)$$

Now σ_{90} will be a minimum when $\frac{\partial \sigma_{90}}{\partial s} = 0$ which gives

$$b = \frac{s^2 K P_s a}{2 \pi^2} \quad (38)$$

Therefore

$$\sigma_{90} = \frac{K P_s s}{4} \quad (39)$$

which for $K = 25$ kv/cm, $P_s = 0.26$ coul/m² and $S = 0.4$ microns, gives

$$\sigma_{90} \sim 6.5 \times 10^{-2} \text{ joules/m}^2 \quad (40)$$

for a 90° wall. We also note that $b \sim 2.1 \times 10^{-18}$ joules.

180° Wall in a Field Normal to the Wall

We refer to the experimental observation that in a 5 kv/cm electric field normal to a 180° wall, there is an unrotated region of about $\frac{1}{2}$ micron width at the wall. We wish to derive this "wall" thickness from the same energy model used for the 90° wall. Here

$$u_i = P_s (K \sin^2 \theta \cos^2 \theta - E \sin \theta) \quad (41)$$

where K is still 25×10^5 kv/cm and E is 5 kv/cm. Under the

same assumptions as before, the surface energy due to rotation of the dipoles from $\theta = 0$ at the wall to $\theta = \theta_1$ in the body of the domain is the sum of

$$\sigma_{u_1} = \frac{s' p_s}{\theta_1} \int_0^{\theta_1} [K \sin^2 \theta \cos^2 \theta - \epsilon \sin \theta - \frac{u_1(\theta)}{p_s}] d\theta \quad (42)$$

and

$$\sigma_{u_2} = \frac{b \theta_1^2}{s' a} \quad (43)$$

where u_2 is again a postulated energy tending to spread out a distortion.

Therefore

$$\sigma_{tot} = \sigma_{u_1} + \sigma_{u_2} = \frac{b \theta_1^2}{s' a} + 0.2 \times 10^5 p_s s' \quad (44)$$

Now let $\frac{\partial \sigma_{tot}}{\partial s'} = 0$ and we find

$$s' \approx \sqrt[3]{b} \sim 0.1 \text{ micron} \quad (45)$$

if $b \sim 2.1 \times 10^{-18}$ as found before. Therefore, the unrotated region should be about 0.2 microns thick, which is the right order of magnitude.

Although these results are approximate, they are a starting point, and a better approach involves internal forces beyond our present knowledge.

LIST OF FIGURES AND ILLUSTRATIONS

<u>Figure</u>	<u>Description</u>	<u>Page</u>
1.	Rectangular pulse generator circuits.	14
2.	Rotation of polar axes near a 180° wall.	16
3.	180° domains in a $[101]$ crystal.	16
4.	Number of pulses required to remove 180° domains.	19
5.	Schematic diagram of 180° domain switching process.	23
6.	Number of 180° domains as a function of field strength.	24
7.	Time required for 180° domains to reverse the polarization of a $[101]$ crystal.	25
8.	Dependence of susceptibility and $\tan \delta$ on field strength and frequency.	28
9.	90° domains; a) 90° wall, b) 90° wall motion	32
10.	90° wedge nucleation, a) positive field, b) negative field, c) 90° wedges.	33
11.	Critical field for 90° wedge nucleation as a function of temperature.	35
12.	Number of 90° wedges nucleated by a square pulse as a function of pulse height and pulse length.	37
13.	Minimum pulse length for nucleation of 90° wedges as a function of pulse height.	38
14.	Successive stages in the formation of a free 90° wall in a $[100]$ crystal.	42
15.	90° wall oscillating at 10^3 cps.	44
16.	90° wall amplitude in AC fields as a function of frequency and field strength. $[100]$ crystal.	45
17.	90° and 180° domains in a $[101]$ crystal.	48
18.	Effect of field parallel to 90° wall for a) head-to-tail wall, and b) head-to-head wall.	48

<u>Figure</u>	<u>Description</u>	<u>Page</u>
19.	90° wall displacement in a DC field as a function of time.	51
20.	Schematic diagrams of 180° and 90° wall interactions in a [101] crystal.	52
21.	Total 90° wall displacement in a DC field as a function of field strength.	56
22.	Total 90° wall displacement caused by a square pulse as a function of pulse length.	57
23.	90° wall displacement in a low frequency AC field as a function of time and field strength.	59
24.	90° wall amplitude in AC fields as a function of field strength and frequency. [101] crystal.	61
25.	Dependence of 90° wall amplitude on temperature.	63
26.	Dense 90° domains at high temperature.	63
27.	Rotation of extinction direction as a function of field strength.	66
28.	Cubic-tetragonal domain walls.	69
29.	Schematic diagram of 90° wedge.	73
30.	Schematic diagram of 180° wedge.	77
31.	Dependence of polarization on Θ .	89
32.	Free energy as a function of polarization.	90

BIBLIOGRAPHY

- (1) E. Wainer, and A. N. Salomon, Titanium Alloy Mfg. Co.
Elect. Rep. 8 (1942), 9 and 10 (1943).
- (2) A. R. von Hippel and co-workers, N.D.R.C. Rep. No. 300
(1944); 540 (1945).
- (3) A. R. von Hippel, R. Breckenridge, F. Chesley, and L. Tisza,
Ind. Eng. Chem. 38, 1097 (1946).
- (4) B. M. Wul and I. M. Goldman, Comptes Rendus (USSR) 46, 139
(1945); B. M. Wul and L. F. Vereschagen, Comptes Rendus
(USSR) 48, 634 (1945).
- (5) H. D. Megaw, Proc. Roy. Soc. 189A, 261 (1947); Trans.
Faraday Soc. 42A, 224 (1946).
- (6) S. Roberts, Phys. Rev. 71, 890 (1947).
- (7) Blattner, Matthias and Mertz, Helv. Phys. Acta 20, 225 (1947).
- (8) Blattner, Matthias, Mertz and Scherrer, Experientia 3, 148
(1947).
- (9) P. W. Forsbergh, Jr., Phys. Rev. 76, 1187 (1949).
- (10) W. J. Mertz, Phys. Rev. 76, 1221 (1949).
- (11) H. F. Kay and P. Vousden, Phil. Mag. (7) 40, 1019 (1949).
- (12) J. G. Powles, and W. Jackson, Proc. Inst. Elec. Eng. 96, III,
383 (1949).
- (13) A. R. von Hippel and W. B. Westphal, Nat. Research Council
Conference on Electrical Insulation, October (1948).
- (14) A. R. von Hippel, Rev. Mod. Phys. 22, 221 (1950).
- (15) J. C. Slater, Phys. Rev. 78, 748 (1950).
- (16) A. F. Devonshire, Phil. Mag. (7) 40, 1040 (1949); 42, 1065
(1951).
- (17) B. Matthias and A. von Hippel, Phys. Rev. 73, 1378 (1948).
- (18) W. J. Mertz, Phys. Rev. 88, 421 (1952).
- (19) L. E. Cross, Proc. Leeds Phil. and Lit. Soc. V(III), 199
(1949).

- (20) A. R. von Hippel, Tech. Rep. 51, Lab. Ins. Res. Mass. Inst. Tech., March 1952.
- (21) T. Mitsui and J. Furuichi, Phys. Rev. 90, 193 (1953).
- (22) J. Hyde, Bachelor's Thesis, Mass. Inst. Tech., June 1954.
- (23) D. R. Young, Private Communication.
- (24) R. Smoluchowski, "Nucleation Theory", Phase Transformations in Solids, John Wiley and Sons, Inc., New York, 1951.
- (25) A. H. Cottrell, Dislocations and Plastic Flow, Oxford, Clarendon Press, 1953.
- (26) M. H. Cohen, Phys. Rev. 84, 369 (1951).
- (27) M. E. Drougard and D. R. Young, Phys. Rev. 94, 1561 (1954).
- (28) W. J. Mertz, Private Communication, June 1954.
- (29) W. G. Cady, Piezoelectricity, McGraw-Hill, New York, 1946.
- (30) W. P. Mason, Phys. Rev. 74, 1134 (1948).
- (31) W. J. Mertz, Phys. Rev. 91, 513 (1953).

BIOGRAPHICAL NOTE

- 1926: Born in Mineola, New York.
- 1932-1944: Attended Cathedral School of St. Mary, Garden City, N.Y.
- 1944-1948: Attended Wellesley College, Wellesley, Mass.
- 1948: B.A. with high honors in physics, Durant Scholar, Phi Beta Kappa, Associate Member of Sigma Xi.
- 1948-1949: Physics Training Program, General Electric Co., Schenectady, N.Y.
- 1949-1950: Research Assistant, Light Production Division, Research Laboratory, General Electric Co.; publication - L.R. Koller and E.D. Alden, "Electron Penetration and Scattering in Phosphors", L. Phys. Rev. 83, 684 (1951).
- 1950: Entered M.I.T. as graduate student in Physics.
- 1950-1952: M.I.T. tuition scholarship.
- 1952: Joined Laboratory for Insulation Research in September.
- 1952-1954: I.B.M. Fellow in Ferroelectric and Ferromagnetic Materials.
- 1954: Member Sigma Xi.